Synthesis and Characterization of Nickel Hydroxide-Impregnated Iron-Based Metal-Organic Framework as Cathode Materials for Supercapacitor Application

Segenet Dagmawi Agegnehu

A thesis Submitted to the Department of Materials Science and Engineering,

School of Mechanical, Chemical and Materials Engineering

Presented in Partial Fulfillment of the Requirement for the Degree of Master's in Materials Science and Engineering

Office of Graduate Studies

Adama Science and Technology University

Jun, 2024

Adama, Ethiopia

Synthesis and Characterization of Nickel Hydroxide-Impregnated Iron Based Metal-Organic Framework as Cathode Materials for Supercapacitor Application

Ms. Segenet Dagmawi Agegnehu

Main Advisor: Dinsefa Mensur (Asso.Prof.)

Co-Advisor: Shimelis Lemma (PhD)

A thesis Submitted to the Department of Materials Science and Engineering,

School of Mechanical, Chemical and Materials Engineering

Presented in Partial Fulfillment of the Requirement for the Degree of Master's in Materials science and Engineering

Office of Graduate Studies

Adama Science and Technology University

Jun, 2024

Adama, Ethiopia

DECLARATION

I hereby declare that this Master Thesis entitled “Synthesis and Characterization of Nickel Hydroxide-Impregnated Iron Based Metal-Organic Framework as Cathode Materials for Supercapacitor Application” is my own work and it has not been submitted for the award of any academic degree, diploma, or certificate in any other university. All sources of materials that are used for this thesis has been duly acknowledged through citation.

Name of student	Signature	Date

RECOMMENDATION

I/we, the advisor(s) of this thesis, hereby certify that I/we have read the revised version of the thesis entitled ‘‘Synthesis and Characterization of Nickel Hydroxide-Impregnated Iron Based Metal-Organic Framework as Cathode Materials for Supercapacitor Application” prepared under my guidance by Segenet Dagmawi submitted in partial fulfillment of the requirements for the degree of Masters of Science in Materials Science and Engineering, Therefore, I/we recommend the submission of a revised version of the thesis to the department following the applicable procedures.

Major Advisor/Supervisor	Signature	Date
Co-advisor/Co-supervisor	Signature	Date

APPROVAL

I/we, the advisors of the thesis entitled “Synthesis and Characterization of Nickel Hydroxide-Impregnated Iron Based Metal-Organic Framework as Cathode Materials for Supercapacitor Application” and developed by Segenet Dagmawi hereby certify that the recommendation and suggestions made by the board of examiners are appropriately incorporated into the final version of the thesis.

_____	_____	_____
Major Advisor/Supervisor	Signature	Date
_____	_____	_____
Co-advisor/ Co-supervisor	Signature	Date

APPROVAL OF BOARD OF REVIEWERS

We, the undersigned, members of the Board of Examiners of the thesis by Segenet Dagmawi have read and evaluated the thesis entitled "Synthesis and Characterization of Nickel Hydroxide-Impregnated Iron Based Metal-Organic Framework as Cathode Materials for Supercapacitor Application" and examined the candidate during open defense. This is, therefore, to certify that the thesis is accepted for partial fulfillment of the requirement of the degree of Master of Science in material science and engineering.

Chairperson	Signature	Date
Internal Examiner	Signature	Date
External Examiner	Signature	Date

Finally, approval and acceptance of the thesis is contingent upon submission of its final copy to the Office of Postgraduate Studies (OPGS) through the Department Graduate Council (DGC) and School Graduate Committee (SGC).

Department Head	Signature	Date
School Dean	Signature	Date
Office of Postgraduate Studies, Dean	Signature	Date

ACKNOWLEDGMENT

I would like to sincerely thank my research advisor, Asso. Prof. Dinsefa Mensur Andoshe, for his insightful comments, which greatly improved and guided the thesis process from reviewing papers to the completion of my work. I would like to express my gratitude to my co-advisor, Shimelis Lemma (PhD), for his support and advice. Additionally, I would like to thank Dr. Gabisa Bekele Feyisa for his encouragement and support in my research pursuit. and, I want to express my gratitude to Sweta Thangriyal for her guidance and mentorship throughout my research and to my family for their unwavering support throughout this protracted trip. Thank you to everyone who helped in the lab and to all of my friends in our department. We wish a special thank you to Mr. Demeke for his unlimited support. Finally, yet importantly, I would like to express my gratitude to Adama Science and Technology University and the Department of Material Science and Engineering for their precious support.

Table of Contents

LIST OF FIGURES

concentrations of electrode materials. 51

Figure 4 10: Capacitance retention vs. cycle number of the MIL-53(Fe), β-Ni$(OH)_2$, M-Ni2 .53

Figure 4. 11: Nyquist plot of MIL-53(Fe), β-Ni(OH)2,M-Ni2 54

LIST OF TABLE

LIST OF ACRONYMS

SCs	Supercapacitors
MOF	Metal-Organic Framework
CP	Conducting Polymer
Cs	Specific Capacitance
PET	polyethylene terephthalic
EDLC	Electrical Double Layer Capacitor
PC	Pseudo- Capacitor
BSSs	Battery Storage Systems
SCDs	Supercapacitor Devices
GC	Glassy Carbon Electrode
CV	Cyclic Voltammetry
CP	Chronopotentiometry
GCD	Galvanostaic Charge-Discharge
EIS	Electrochemical Impedance Spectroscopy
Rct	Charge Transfer Resistance
Rs	Series Resistance
XRD	X-Ray Diffraction
FTIR	Fourier Transform Infrared Spectroscopy
SEM	Scanning Electron Microscopy
BET	Brunauer, Emmett, and Teller
PET	polyethylene terephthalate

ABSTRACT

Supercapacitors, also known as electrochemical capacitors, are devices used for storing energy that fills the gap between conventional capacitors and batteries. They are known for their high power density, quick charging and discharging cycles, and long life span. They are well suited for applications, including portable electronics, electric vehicles, and grid energy storage. Importantly, supercapacitors' performance depends on the materials used for electrodes. Nickel hydroxide is widely recognized for its excellent redox properties and high specific capacitance, making it a promising electrode material for supercapacitors. However, several challenges hinder its application. Making hybrid materials is the best option to increase the capacitance of electrode material and to overcome the limitation of a single electrode material. The combination of high surface area and structural benefit of metal-organic framework (MOF) with the excellent redox properties of transition metal hydroxides is the best candidate electrode material. In this study, MIL-53(Fe)/β-$Ni(OH)_2$ nanocomposites were synthesized through the Sonochemical Wet Impregnation assisted method in the ratio of (10, 20, 30% of $Ni(OH)_2$), and their names are assigned as M-Ni1, M-Ni2, and M-Ni3 respectively. Characterization techniques such as X-ray diffraction, Brunauer, Emmett, and Teller, scanning electron microscopy, Fourier transform infrared spectroscopy, cyclic voltammetry, galvanostatic charge-discharge, and electrochemical impedance spectroscopy were used. The effect of varying the $Ni(OH)_2$ concentration on the electro-performance of the composite has been exploited. Among the investigated concentrations, 20% $Ni(OH)_2$ impregnated MIL-53(Fe) which is an iron-based metal-organic framework with terephthalic acid as an organic linker exhibited the highest areal capacitance of 2.2F/cm^2 at 1 mA/cm^2 current density and 99.2% of capacitance retention in an aqueous Na_2SO_4 electrolyte. This superior performance is attributed to the optimal encapsulation of $Ni(OH)_2$, which enhances the active surface area and leverages the synergistically with other components, improving overall performance through mechanisms like facilitated ion transport effect between β-$Ni(OH)_2$ and the MOF work.

CHAPTER ONE

1. INTRODUCTION

1.1. Background

Accessing safe, sustainable, and economically viable energy is vital for individual prosperity and civilization. Societal growth in modern times through history, humans have utilized diverse energy sources, including wood, coal, oil, gas, and biomass, and recently, harnessed the power of the sun, wind, and water for cooking by electricity generation, and energy production(Patrice Simon & Yury Gogotsi, 2008). Despite the availability of abundant energy resources, the challenge of accessing sustainable and clean energy remains significant. The current energy market heavily relies on non-renewable energy sources. Overdependence on coal, oil, and gas for energy leads to excessive depletion of natural resources. Greenhouse gases (CH_4, CO_2) and pollutants primarily originate from fossil fuel combustion (White et al., 2015). Fossil fuel consumption as the main energy source is harmful to social complexity and environmental sustainability (R. Xiong et al., 2020).

Renewable energy sources, including solar power, wind power, hydropower, geothermal, and biomass, offer a clean alternative with the potential to significantly reduce our reliance on fossil fuels and mitigate environmental pollutants. Renewable energy resources such as sun power and wind power can have inconsistent generation and peaks that do not correspond with energy demand. The increasing uncertainty in energy supply and demand is raising concerning about their reliability.

Future energy systems require an essential integration of energy resources in households, industry, and transportation through the widespread replacement of internal combustion engines with low/zero emission vehicles. A diverse range of energy storage systems in multiple configurations is essential. Various applications have led to the development of several energy storage technologies.

Energy storage technology is led by electrochemical energy storage. From portable electronics to hybrid vehicles, technology plays a significant role in our daily lives. Electrochemical energy storage devices include electrochemical secondary batteries, fuel cells, and supercapacitors. The technological advantages of each type are unique (M. Winter & R. J. Brodd, 2004). Both lithium-ion batteries and fuel cells offer high energy densities but power delivery limitations for certain applications. Supercapacitors have recently attracted much interest owing to their unique abilities to deliver high power release or uptake (10 KW) in very short times (a few seconds). supercapacitors, which can store hundreds or thousands of times more charge than conventional electrostatic capacitors, are more appealing for meeting practical energy storage demands (Liu et al., 2009).

Platinum group metal-based electrodes have been acknowledged as the most efficient electrode materials for supercapacitor applications. However, their high cost and scarcity hinder their widespread use in large-scale hydrogen production. It is crucial to reduce the reliance on noble metals and instead utilize abundant non-noble metal alternatives that exhibit exceptional catalytic performance and durability. Transition metal oxides and hydroxides such as $NiO/Ni(OH)_2$, $Co_3O_4/Co(OH)_2$, $Fe_2O_3/FeOOH$, and MnO_2 can used as electrode materials for electrochemical energy devices (Cao et al., 2022). Among them, nickel hydroxides have the best redox reaction, have the highest specific capacitance but have limitations like long-term stability, cycle stability because of mechanical instability, and insufficient structure (Wang et al., 2019). MOFs have garnered significant attention for supercapacitor applications due to their structural properties. MOFs consist of metal ions to organic linkers, forming highly porous and crystalline materials. This porosity provides an exceptionally high surface area, which is crucial for enhancing the electrochemical performance of supercapacitors. In addition to the surface area and porosity, the metal ion and the carbon on the linker influence to attend a good specific capacity and the synergetic effect when making a composite significantly increases its performance (Cao et al., 2022; Sundriyal et al., 2018). Organic ligands act as a linker connecting the MOF skeleton, therefore, the organic ligands are also known MOFs linkers. Special connections between metal ions/clusters and MOFs linkers lead to a theoretically unlimited number of MOFs with different structural and properties. When designing MOFs, linkers design is one of the most important factors due to the unlimited possibility to design functional or multi-functional MOFs linkers as well as distinctive chemical properties of organic functional groups.

The MOF linkers can be classified based on their functional group into the following six major categories including carboxylic MOF linkers, nitrogen MOF linkers, phosphorous MOF linkers, sulfonic acid MOF linkers, halogen MOF linkers, hydroxyl MOF linkers. Carboxylate linkers-based MOFs have remarkably high surface area and uniform pore size distribution, highly ordered crystallinity. In this, study Terephthalic acid, which is one of the carboxylic acids, is used as a linker that is recycled from waste polyethylene terephthalate water bottles.

1.2. Statement of the problem

Nickel hydroxide ($Ni(OH)_2$) is widely recognized for its excellent redox properties and high specific capacitance, making it a promising candidate for supercapacitor electrode material. However, several challenges hinder its application (Lee et al., 2017). $Ni(OH)_2$ have low mechanical stability and low chemical stability (Wang et al., 2019), and also surface area and porosity relatively low compared to the other carbon-based materials used in supercapacitors (Raza et al., 2018). To address these limitations an integration of $Ni(OH)_2$ with different materials can enhance its stability, and surface areas to have more active sites for electrochemical reactions to occur (Tonelli et al., 2021). One promising strategy is combining a high surface area and porous material like a MOF which can mitigate these drawbacks and improve its suitability for advanced supercapacitor applications. The iron-based MOF is a potential electrode material for supercapacitors due to its good capacitive properties of FeOH metal node and excess carbons in terephthalic acid from the organic linker which recycled from waste polyethylene terephthalic (PET) known for water bottle, helps in order to avoid environmental pollution specifically soil pollution caused by waste PET (Chameh et al., 2021). MIL-53(Fe) offers excellent chemical stability, high porosity, and large surface area, which can enhance the desperation and stability of β-$Ni(OH)_2$. By impregnating β-$Ni(OH)_2$ into the MIL-53(Fe) framework, we aim to overcome its inherent limitations, thereby improving its electrochemical performance, stability and also enhances conductivity through the combination of $Ni(OH)_2$ for supercapacitor application through a synergetic effect and by impregnating the metal hydroxide into MOF.

1.3. Objective

1.3.1. General objective

Synthesis and characterization of nickel hydroxide- impregnated iron based organic framework as cathode for supercapacitor application.

1.3.2. Specific objective

- ✓ To Extract terephthalic acid from a waste plastic bottle
- ✓ To synthesize MIL-53(Fe)
- ✓ To synthesize β-$Ni(OH)_2$ from Nickel nitrate hexahydrate ($Ni(NO_3)_2 6H_2O$)
- ✓ To prepare MIL-53(Fe)/β-Ni $(OH)_2$ composite
- ✓ To characterize of structural, surface morphology and surface area, pore volume and size of MIL-53(Fe), β-$Ni(OH)_2$, MIL-53(Fe)/$Ni(OH)_2$ composite
- ✓ To investigate the electrochemical performance of MIL-53(Fe), β-$Ni(OH)_2$, MIL-53(Fe)/β-$Ni(OH)_2$ composite using Cyclic voltammetry (CV), Galvanostatic charge-discharge (GCD) using Chronopotentiometry technique, and electrochemical impedance spectroscopy (EIS).

1.4. Significance of the study

Fossil fuels are used extensively worldwide this days, but they have given rise to a number of issues that might be summed up as an energy crisis(Armand & Tarascon, 2008). New forms of clean intermittent energy sources like solar and wind power are always being developed (Choi & Aurbach, 2016). However, the majority of these new energy sources are inconsistent, which continues to be challenging for the reliable operation of the power system. One important strategy for resolving this issue is the use of energy storage technologies. Among the energy storage technologies, the potential of supercapacitors to transform energy storage technology and close the gap between traditional batteries and capacitors makes their study extremely important (Lu et al., 2013).

Supercapacitors have several distinct advantages, including long cycle life, high power density, quick charge and discharge cycles, and exceptional efficiency. Their characteristics render them perfect for a wide range of uses, encompassing consumer electronics, electric automobiles, and sustainable energy systems (Du et al., 2020; Karthikeyan et al., 2021).

Development in supercapacitor technology could result in breakthroughs in energy resource management, improving the functionality of electronic products, and assisting in the shift to a low carbon economy as the need for effective, dependable, and sustainable energy storage solution increases. The development of more robust and flexible energy storage systems that can fulfill the rising energy demands requires an understanding of and improvement upon supercapacitors (Nagarajarao et al., 2022).

1.5. Scope of the study

This research explores the synthesis, characterization, and performance evaluation of nickel hydroxide to Iron-based MOF composites for supercapacitor applications. The main objective is to explore the synergetic effect of impregnating nickel hydroxide to Fe-MOFs, understand their electrochemical properties, and assess their potential to enhance energy storage capabilities. In this study, β-$Ni(OH)_2$ and Fe-based MOF are used as potential electrode materials for supercapacitor application. Co-precipitation, wet chemical ultrasonic assisted synthesis was used to synthesize the MIL-53(Fe)/β-$Ni(OH)_2$ composite and then characterize chemical composition, crystal structure, crystallinity, surface area, pore size, and surface morphology and its electrochemical performance using different techniques, including cyclic voltammetry (CV), chronopotentiometry (CP), electrochemical impedance spectroscopy (EIS).

CHAPTER TWO

2. LITERATURE REVIEW

2.1. Global energy status

The welfare, economic, and developmental states of societies are based on energy. Fossil fuels, notably oil, coal, and gas, account for around 85% of the primary energy used by humans and are the predominate primary energy sources (Dehghani-sanij et al., 2015) According to keith and krumdieck (2013),0 the world's population is expected to increase and reach about 9 billion by 2048. New renewable energy sources must be developed (Dehghani-Sanij et al., 2017). Particularly in developing nations with large populations, industrialization, and economic explanation all contribute to rising energy consumption (Bahadori & Dehghani-sanij, 2014; Mohamed et al., 2015; Sb, 2015; Soltani et al., 2018). Growing demand brings environmental problems like climate change and global warming, the health effects of air pollution, and the possibility of contaminated soil and water (Guney & Tepe, 2017; Pérez-Lombard et al., 2008).

Concerns regarding energy resource depletion, supply constraints, and adverse environmental effects (ozone layer depletion, global warming, climate change, etc.) have already been brought up by the world's rapidly expanding energy use. The international energy agency has compiled data on trends in energy usage that are alarming. Primary energy has increased by 49% and CO_2 emissions by 43% over the past 20 years (1984-2004), with average annual increases of 2% and 1.8%, respectively. Predictions for the future indicate that this increasing trend will continue (Pérez-Lombard et al., 2008).

In the last few decades, energy storage technologies have come to play an important role as far as the electric grid is concerned. The fact that there are a growing number of different applications that need a specific power or voltage level in a short amount of time is one of the key causes of this (Boicea, 2014). A set of techniques and tools used to store energy is known as an energy storage system. Later on, the stored energy can be used to carry out beneficial tasks.

Despite not being energy sources, energy storage technologies offer significant benefits that enhance supply reliability, stability, and power quality. The challenges of practical electric vehicles and utility used have been meeting by substantial advancements in battery technologies. Modern, non-polluting uninterruptible power supplies employ flywheel technology. In order to store energy for power quality applications, advanced capacitors are being studied. Utility applications are drawing attention to superconducting energy storage devices, which are still in the prototype stage (Ribeiro et al., 2001).

2.2. Electrochemical Energy Storage Systems

2.2.1. Battery storage system (BSSs)

An electrochemical battery is made up of two or more cells that can transform chemical energy into electrical energy. These serve as tools for storing and converting energy. Its limited fuel and oxidant supply means that electrical energy can be generated momentarily(Martin Winter & Ralph J Brodd, 2004). For a battery to operate smoothly, electrodes (such as the metal zinc, lead, and lithium) need to have high surface areas, strong electrical conductivity, and compatibility with the electrolyte(Weiss et al., 2021). Primary batteries, like lithium batteries, and secondary batteries, like lithium-ion batteries, are two different types of batteries. The latter is rechargeable, but the former is not (it is metallic). Li-ion batteries are not as energy dense as non-rechargeable batteries, but they still provide a high load current. Anode, cathode, separator, and electrolyte are the components of both (Kurzweil & Chwistek, 2008; Winter et al., 1998).

Currently, batteries are an integrated part of our daily routines. In certain respects, batteries exhibit drawbacks. It covers, less power density is the problem hinders its higher discharge of power, and a rate of recharge is required and Safety concerns and heating effects many batteries have flammable, corrosive, non- eco-friendly, and toxic electrolytes and the reduction and oxidation reaction produce heating effect in batteries during their usage (Sivanantham et al., 2021). Battery cycle lives are inherently limited due to the reduction and oxidation reactions. The highlighted, issues hinder batteries from providing a comprehensive solution for electrical energy storage.

An ending, secure electrical energy storage system bosting superior energy and power capabilities would transform energy production, transmission, and consumption. In the electrical power industry, dependable power systems remain essential for consumers, industries, and defense force (Arbizzani et al., 2001; Arulepp et al., 2006; Burke, 2011; Omanda et al., 2004)

2.2.2. Fuel cell

Fuel cells change chemical energy into electricity as needed. In fuel cells, the anode undergoes oxidation, the cathode undergoes reduction, and the electrolyte facilitates current flow through ion conduction (Mekhilef et al., 2012). In contrast to batteries, fuel cells receive their oxidants and fuel from external sources. Like internal combustion engines, fuel cell function only with a continuous fuel supply. Fuel cells are not electrically recharged; instead, they are refueled after use operational perspective considers hydrogen gas as the preferred fuel due to water exhaust. Hydrogen require for fuel cells when converting other fuels and hydrocarbons. Under certain conditions fuel cell electrodes can directly convert fuels like methanol and methane instead of batteries (Haile, 2003; Wang & Jiang, 2017). These functions include maintaining a stable gas electrolyte interface, catalyzing the electrode reactions and transferring electrons to/from the reaction sites. The three-phase boundary, where the electrolyte, electrode, and gas converge, poses a major challenge in controlling the interface. A stable three-phase boundary ensures optimal performance and prolonged operation. The porosity electrolyte- electrode contact must be precisely controlled (Hirchenhofer et al., 1998).

2.2.3. Supercapacitor

The mechanism of energy storage in supercapacitors (SCs), also known as electric double layer capacitor (EDLC) or ultracapacitors, involves a simple charge separation at the interface between the electrode and the electrolyte. This allows the devices to store and deliver energy at relatively higher rates than batteries SC have a very high capacity and low internal resistance (Lu et al., 2020; Stoller et al., 2008). An electrolyte, two electrodes, and a separator that electrically isolates the two electrodes make up a SC. The most crucial element of a SC is the electrode material (Mohammed et al., 2021; Pope et al., 2013). When compared to other energy storage technologies, SC have a number of advantages, including a long lifespan, high power, flexible packaging, a wide temperature range (-40 to 70 ˚C), low maintenance, and low weight (Wang et al., 2009).

The majority of renewable energy sources, with the exception of bio-fuels, are supplied as electricity. A dependable technological platform for electrochemical storage, such as batteries, fuel cells, and electrochemical supercapacitors, has been in high demand (Czagany et al., 2024; Tasnin & Saikia, 2018). Specifically, quick storage capacity (i.e.,. short discharge time: SC: 1-10 s vs. lithium ion battery: 10-60 min) and improved cyclic stability (SC > 30,000 h vs. battery > 500 h) have attracted a greater attention to supercapacitors than batteries (Panda et al., 2020). Beyond low energy density, recent developments in supercapacitors concerning electrode materials and electrolytes have the ability to bridge the gap between current electrolyte capacitors technology and that of batteries and fuel cells (Raza et al., 2018).

SCs have emerged as viable options in a variety of industries that demand high energy throughput (hybrid electric vehicles) and stable energy throughput (sensitive automation, computer chips, and portable electronic devices),in line with resent technological advancements in electric-powered devices in terms of cycle life, charge time, and specific power. supercapacitors are energy storage devices with very high capacity and low internal resistance, that are able to store and deliver energy at relatively higher rates as compared to batteries due to the mechanism of energy storage which involves a simple charge separation at the interface between the electrode and electrolyte interface (Choi & Aurbach, 2016; Stoller et al., 2008; Wu et al., 2010).

A SC is a pulse current system that is intended to address short- term requirement of less than one minute for high current and specific power (10,000 W Kg^{-1}). As a result, SCs can be utilized alone or in conjunction with batteries or another form of energy storage to provide increased cycle life and power efficiency for applications like trains, elevators, hybrid vehicles, and cranes (Carignano et al., 2017; Kerns, 2015; Song et al., 2017). The first patent application and issuance for a prototype SC occurred in 1957. The market for SC technology was not very strong outside of the hybrid electric car industry until the 1990s (Kötz & Carlen, 2000).

The goal of current, comprehensive SC technology development is to improve electrode materials' electrical performance (Deka et al., 2017). Different kinds of SCs are already being utilized in drive system that draw power from a voltage source to meet the power requirements for initiating and recovering braking energy (Hartmann et al., 2017; Lu et al., 2017). Consequently, SCs are a good choice for a variety of energy storage applications, such as serving as backup power sources to guard against power outages(Patrice Simon & Yury Gogotsi, 2008; Wang et al., 2012)

Batteries are the sources of energy for day lasting instrument and for the day lasting instrument. SCs are utilized. In hybrid vehicles, SCs recover and store heat power for passenger and cargo usage during regenerative breaking SCs have a comparatively lower energy storage capacity, per unit mass or area, than other types of batteries. Both supercapacitors and batteries are based on electrochemical reactions. Research on materials for high energy capacity batteries has bombed alongside that for SCs boasting eternal energy yet low recharging rate (Holze, 2015). The unique charge storage capabilities of batteries and SCs stem from their distinct electrochemical reactions. Lithium ions in bulk electrodes cause slower and controlled reduction and oxidation reactions through diffusion. SCs or electric double layered capacitors store charges via electrolyte ion adsorption onto the electrode materials (Holze, 2015). The response's potential change occurs more quickly with high power levels (Simon & Gogotsi, 2013). SCs and batteries can be differentiated through the application of galvanostatic and potentio-static techniques.

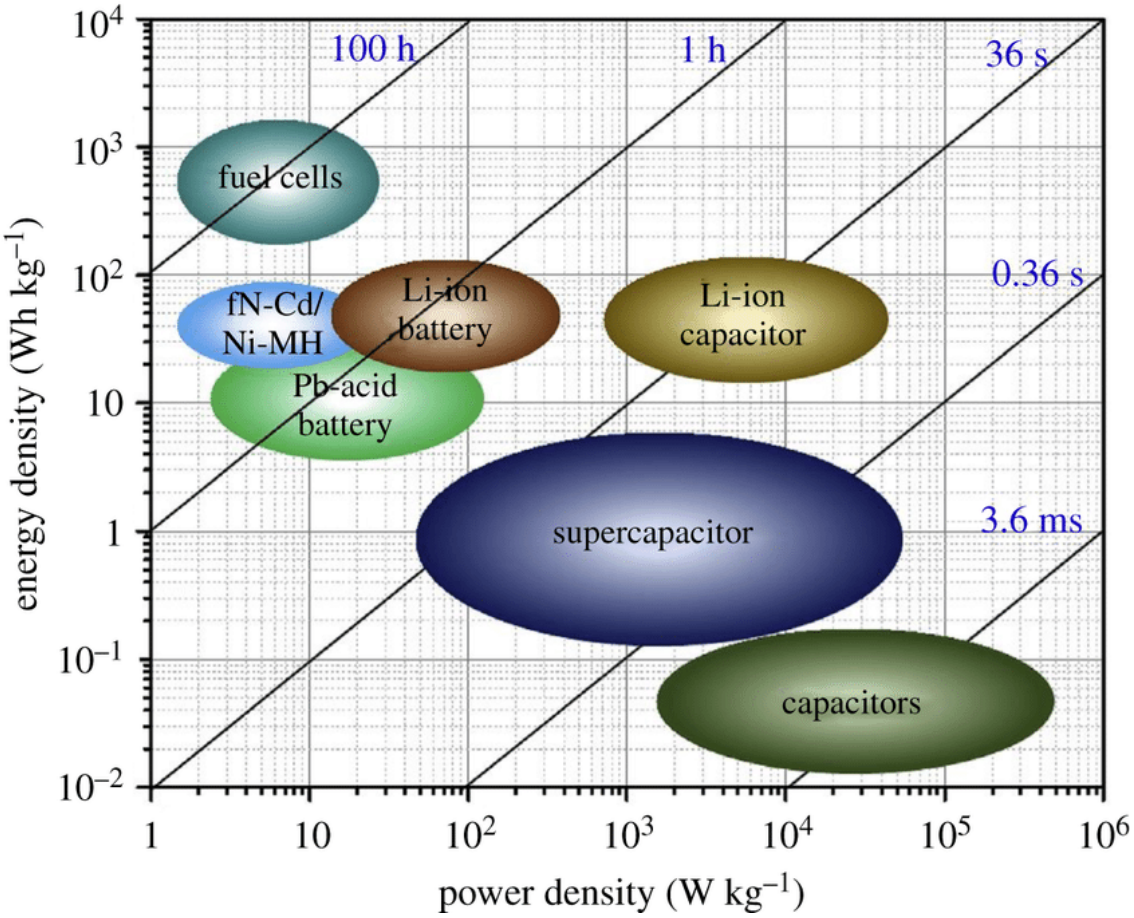

Figure 2. 1: Ragone plot- comparison of the performance of different energy storage devices (Hlongwa & Raleie, 2022)

2.3. Energy storage mechanisms in supercapacitor

Three different capacitive behaviors can be used to explain how energy is stored in SCs: (1) electrochemical double layer capacitors (EDLC) use the pure electric charge that builds up at the electrode interface; (2) pseudo-capacitance (PC) arise from rapid and reversible surface redox process; and (3) hybrid capacitors utilize both mechanisms (Raza et al., 2018).

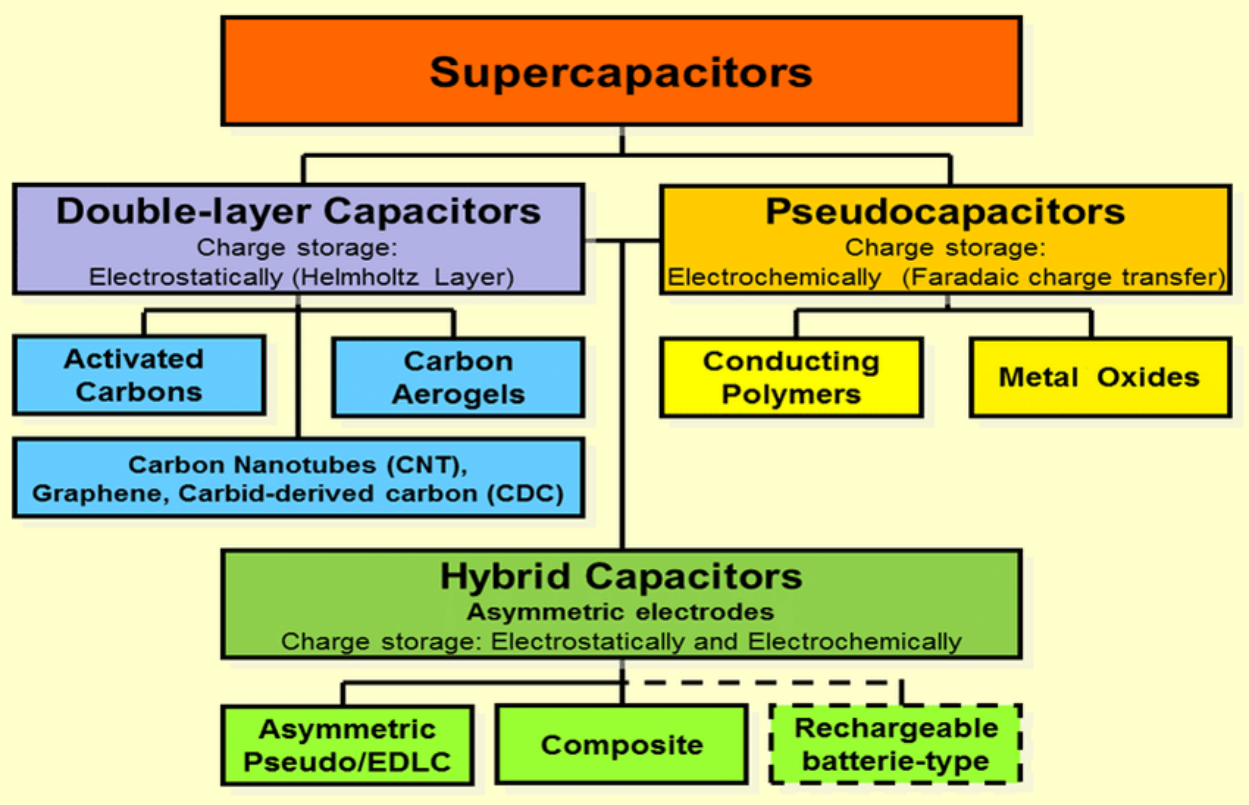

Figure 2. 2: supercapacitor types; electrochemical double-layer capacitors and pseudocapacitors as well as hybrid capacitors are defined over their electrode designs (Oyedotun, 2018)

2.3.1. Electrochemical double-layer capacitor

The first US patent on the EDLC design, filed in the 1950s (Kötz & Carlen, 2000), outlines the use of carbon with a large surface area , applied to metal current collector and submerged in sulfuric acid electrolyte, to facilitate the collection of polarized charges as the foundation for supercapacitor technology. It began commercializing aqueous- electrolyte capacitors in the 1970s, leading their widespread application in energy storage and the emergence of supercapacitors in commercial devices (Kötz & Carlen, 2000).

An EDLC is a type of electrochemical capacitor that electrostatically stores charge by reversible adsorption of electrolyte ions onto electrochemically stable and high surface-area active materials, which separates charge at the electrode-electrolyte interface upon polarization (P. Simon & Y. Gogotsi, 2008).

In an electrolyte and under the influence of an external electric field, the electrode's surface and the electrolyte spontaneously organize charges, forming an electrochemical double layer. Figure 2.3 depicts the schematic of the charge collection process. The charged layers at the electrode surface and in the electrolyte function as a dielectric capacitor, storing energy. In a dielectric capacitor, the insulating barrier is replaced by an electrolyte in a supercapacitor. In an EDLC, electrical energy is stored as surface charges on the electrode material. Superior performance can be achieved through the utilization of electrochemically stable electrode materials boasting high surface area and conductivities. Conductive carbon materials, with their low cost, excellent processing capabilities, superior electrochemical stability, and excellent conductivity, are the optimal choices. Researching capacitive energy storage focuses on discovering carbon materials with substantial surface area is also way to increase stability and performance.

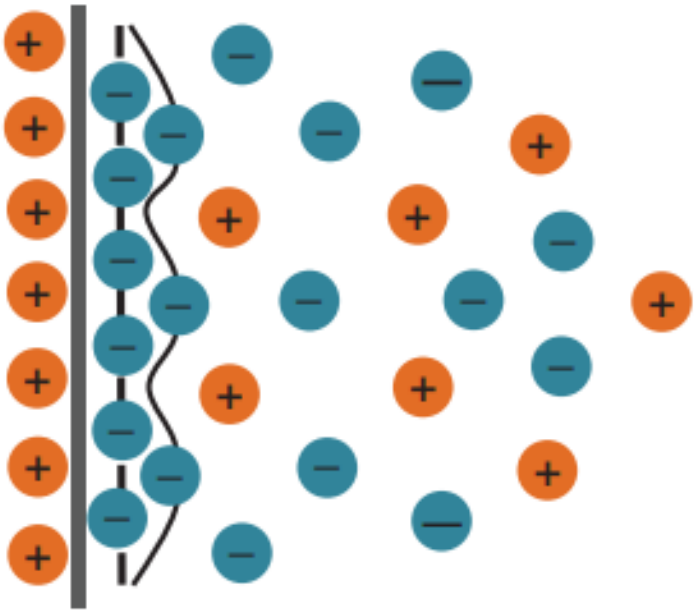

Figure 2. 3: schematic drawing of the basic capacitive mechanisms: electrochemical double-layer principle.

Understanding the double-layer mechanism is essential for designing effective porous carbon electrodes (Chmiola, Yushin, Gogotsi, et al., 2006). Before the proposal of this mechanism, it was generally accepted that pores in the sub-nanometer regime would not be accessible for hydrated ions in aqueous electrolyte, especially in the case of solvated ions in organic electrolyte since the size of these 'energy carriers' is larger than 1 nm (Kim et al., 2004; Qu, 2002). Thus not beneficial for improving the capacitive performance in an EDLC. Several studies have shown conflicting experimental results indicating that carbide-derived microporous carbon electrodes with sub-nanometer pore sizes increase capacitance in capacitors (Chmiola, Yushin, Dash, et al., 2006; Alar Jänes et al., 2004). A de-solvated process must occur before the electric double-layer can form and decrease the size of solvated ions to meet absorption conditions in microporous electrodes.

2.3.2. Pseudocapacitance

In contrast to EDLCs, PCs store charge in the electrode materials through a faradaic process, which involves surface or near surface fast reversible redox reactions (Yu et al., 2018). According to Conway's revised theory on PCs, they have a charge storage mechanism consisting of underpotential deposition, redox pseudocapacitance, and intercalation pseudocapacitance.

The underpotential deposition process entails faradic absorption or desorption of metal ions on various metal surfaces, including Ru, Pt, Au, and Rh, to create an adsorbed monolayer above their redox potential, as shown in fig. 2.4 (d) (Herrero et al., 2001).

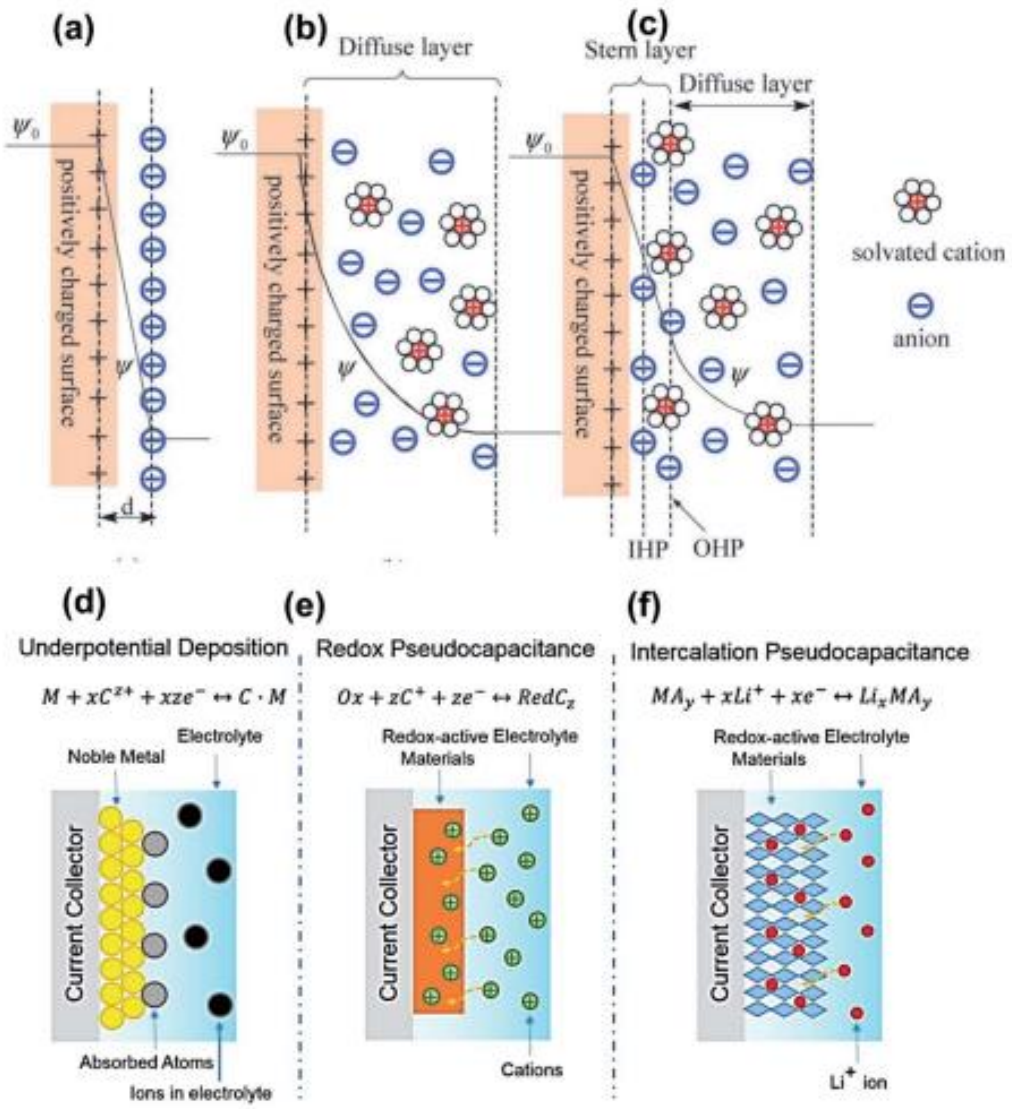

Figure 2. 4: Models of the electrical double layer: (a) Helmholtz model, (b) gouy- chapman model, and (c) stern model, (d) underpotential deposition, (e) redox pseudocapacitance, and (f) intercalation pseudocapacitance (Patra et al., 2021).

Redox pseudocapacitance transpires on material surfaces or nearby due to the coincident faradic charge transfer process, illustrated in Fig.2.4 (e) (Wang et al., 2018). Intercalation pseudocapacitance represents the insertion of ions into the tunnels or sheets of a redox- active electrode material, which stems from the faradic charge transfer process but does not encompass a crystallographic phase change, as depicted in Fig. 2.4 (f) (Gui et al., 2022). PCs incorporate three distinct charge storage mechanisms, each with unique physical processes and electrode materials. The charge storage mechanism in PC electrodes relies on this equation.

$$E \sim E - \frac{RT}{nf} In \frac{X}{1-X} \quad \text{---------- (2. 1)}$$

Commonly used electrode materials in pseudocapactors include RuO_2, IrO_2, NiO, Co_2O_3, SnO_2, V_2O_5, MoOx, MnO_2, Metal hydroxides, metal chalcogenides, conducting polymer-based materials. RuO_2 and MnO_2 are mostly extensively studied as pseudocapacitive electrodes (Gui et al., 2022). Polypyrrole, polyaniline and polythiophene, with their high conductivity, are used as pseudocapacitive electrodes in conducting polymers.

Different types of charge storage exhibit distinct cyclic voltammetry and charge-discharge profiles. The energy storage mechanisms depicted in Fig, 2.5 (a) are illustrated (Gogotsi & Penner, 2018) Capacitve electrode materials display rectangular cyclic voltammogram and linear voltage response during constant current charging-discharging, as depicted in their Type-A cyclic voltammograms and charge- discharge profiles. Similarly, Type-B pseudocapacitive is faradic in nature, while Type C faradic is not capacitive in behavior, namely it is basically battery type (Zhu et al., 2015)

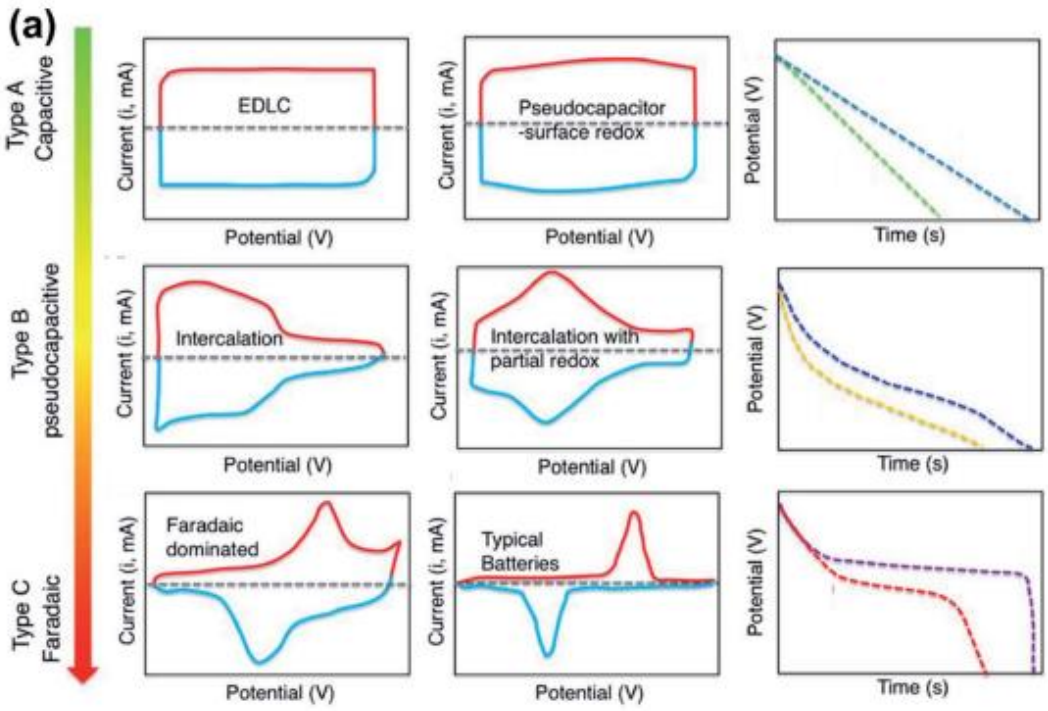

Figure 2. 5: Cyclic Voltammograms and corresponding Charge-Discharge profiles for various types of energy storage materials (Patra et al., 2021).

In recent decades, the surface redox mechanism has gained widespread recognition and is operative in all sorts of pseudocapacitive electrodes. Figure 2.5 illustrates this mechanism. Capacitance is formed in a pseudo- capacitor through faradic redox reactions between the electrolyte ions and the electrode, which store electric energy. In capacitors, unlike batteries, the bulk of the electrode dose not engage in electrochemical reactions, preventing crystallographic and structural changes for heightened cycling stability. Because the surface redox reactions occur only in the top few nanometers in the electrode's surface, nano engineering techniques play a significant role in enhancing pseudo-capacitive properties. Common approaches include decreasing the particle size to improve active materials usage (A. Jänes et al., 2004) and producing nanostructured electron conductive networks for pseudo-electrodes, ultimately to increase their conductivity and this promote power delivery (Du et al., 2019).

Commonly used electrode materials for surface redox mechanisms include metal oxides (RuO_2, MnO_2, NiO, Co_3O_4, Fe_3O_4, V_2O_5), metal hydroxides ($Ni(OH)_2$, $Co(OH)_2$), and conductive polymers. Different electrolyte ions undergo distinct redox reactions. The performance of supercapacitors is significantly influenced by this factor in terms of specific capacitance, power density, and working voltage window.

2.3.3. Hybrid- Capacitors

EDLC offers good cyclic stability, and efficient power performance on the other hand, pseudo capacitance provides greater specific capacitance. In the case of a hybrid system, a combination of both can be achieved by using a battery-like electrode for energy sources and a capacitor-like electrode for power sources in the same cell (Burke, 2007; Burke & Zhao, 2015; Naoi & Simon, 2008). By choosing the right electrode combination, it is possible to increase the cell voltage, resulting in improved energy and power densities. Various combinations of positive and negative electrodes have been tested in aqueous and inorganic electrolytes. However, it is important to note that although the faradic electrode increases energy density, many compromise cyclic stability, which is a major drawback of hybrid devices compared to EDLCs.

2.3.3.1. Composite

A single composite electrode incorporates carbon-based materials, along with metal oxides or conducting polymers, resulting in the integration of both physical and chemical charge storage mechanisms. Due to their capacitive double-layered charge and high specific surface area, carbon-based materials enhance the interaction between pseudocapacitive materials and the electrolyte. Pseudocapacitive material enhances capacitance through faradic reaction within a composite electrode (Ragupathy et al., 2009).

2.3.3.2. Asymmetric

Asymmetric hybrids combine non-faradic and faradic processes by coupling and EDLC with a psuedocapacitor electrode. They are set up in a way that the carbon material is used as a negative electrode while either metal oxide or conducting polymer as positive electrode (Burke, 2007).

2.3.3.3. Battery type

In battery type hybrids, a supercapacitor electrode is integrated with a battery electrode. This configuration utilized the properties of both supercapacitors and batteries with a single cell (Schneuwly & Gallay, 2000).

2.4. Materials systems for supercapacitor

2.4.1. Carbon-based materials

Carbon is a material whose porosity is easy to develop by different existing carbonated structures (sp_2, sp_3). It is the main electrodes active materials used for the EDLC supercapacitors. It has also good electronic and stable conductor electrochemically in a wide range of potential (~3 V). The carbon in different forms has been tested as an electrode for supercapacitors (Lu et al., 2014; Pandolfo & Hollenkamp, 2006; Y. Zhang et al., 2015), including carbon nanotubes, graphene sheets, carbon onions, fibers (Frackowiak & Beguin, 2001), carbon blacks (Inagaki et al., 2010), carbide-derived carbons (Ishikawa et al., 1996), or activated carbons (Krause et al., 2011). These are the latter mainly used as active materials in supercapacitors because they have a very high specific surface area, electrical conductivity in the order of 50 $S.cm^{-1}$, good thermal stability, excellent corrosion resistance for a moderate cost (Chmiola et al., 2005).

2.4.2. Conducting polymers

Conducting polymers have a higher specific capacitance than carbon materials. Conducting polymers are also known as synthetic metals, with conductivities ranging from 1 to 100 $S.cm^{-1}$ (Barbieri et al., 2005). The planar structure of these molecules arises from the series of saturated and unsaturated bonds between their sp^2 hybridized carbon atoms. This configuration facilitates both good electrical conductivity and the recovery of carbon orbitals, enabling π-type hybridization. The orbitals' strong conjugation is the cause of electrical conductivity. Pseudo-capacitive materials exhibit faradaic reactions and continuous potential variation due to the introduction of charges in the polymers. The electrochemical reaction with a conductive polymer electrode results in doping/dedoping due to electron injection or removal. Upon doping, the electrolyte ions inserted into the polymer chain maintain local electroneutrality. "N doping" refers to the reduction reaction while "P doping" refers to the oxidation reaction (Snook et al., 2011).

2.4.3. Metal-organic framework (MOF)

Metal-organic frameworks, often known as MOFs, are a new class of inorganic-organic hybrid materials that have attracted growing interest over the past 20 years (Férey, 2008; Kitagawa et al., 2004; Li et al., 1999; Tranchemontagne et al., 2009). MOFs are made of metal ions or metal clusters and multi-dentate organic linkers. The linkers/organic linkers are basic components used in the production of MOFs terephthalic acid, imidazolates, amines, carboxyl phosphates, and other compounds are examples of these building blocks-ligands (Xiaobo et al., 2021). The linkers give MOFs more moieties or functionalities, such as hydroxyl, carboxyl, sulphonic, phosphate, and amino, are added to MOFs by this linker.

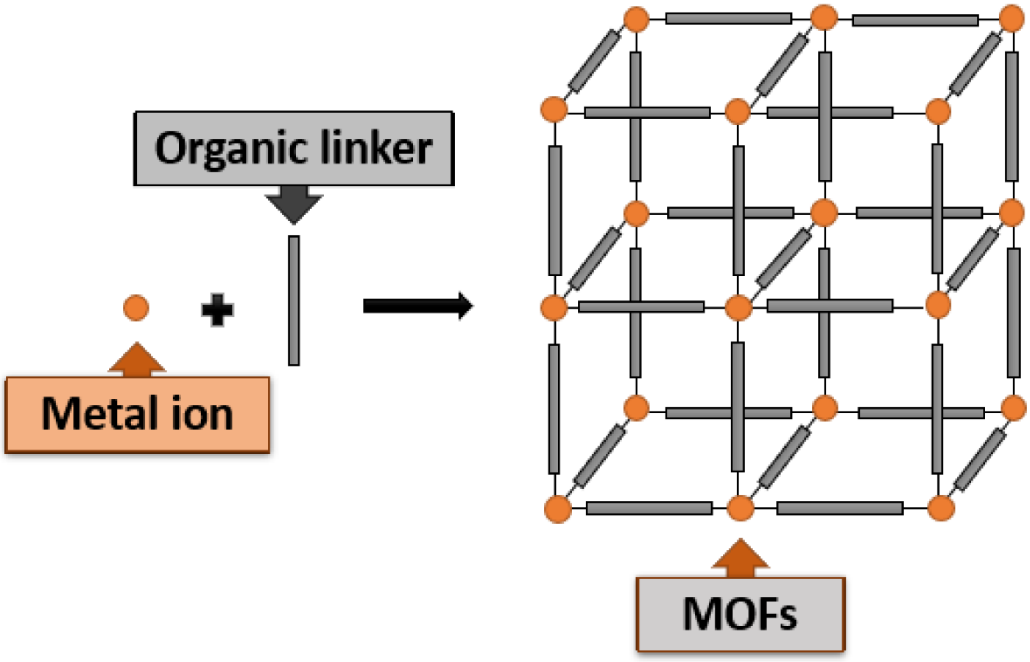

Figure 2. 6: Schematic diagram of the synthesis procedure for MOFs (Naser et al., 2023).

MOFs have the potential to be used in a variety of fields, including wastewater treatment (Granato et al., 2012; Sotnik et al., 2015; Wee et al., 2011; Yepez et al., 2015), catalyst, gas storage and separation, an electrochemical energy storage system (Li et al., 2019; Llewellyn et al., 2008; Trung et al., 2010), luminescence (Yang et al., 2007; Zhang et al., 2017), medicine (Chen et al., 2012; Xie et al., 2015), and sensor (Dargahi et al., 2018; Mahmoodi et al., 2018; Shafiei et al., 2018). This is due to their large surface areas, tunable pore size and structures, light harvesting property, excellent charge transport and abundant active sites.

MOFs are a relatively new class of porous crystalline compounds which have outstanding material properties of high specific surface area, structural tailorability, and permeability to guest molecules (Dai et al., 2012; Dubal et al., 2013). As the synthesis of MOFs proceeds through the reaction between metal ions (or their clusters) and organic linkers, the judicious selection of such components can provide application-specific properties (Kumar et al., 2015). Further, the availability of a large variety of metal ions and organic linkers has facilitated the creation of several thousands of MOFs with various functionalities. As such, MOFs have been adopted in diverse fields of advanced technological applications, including drug delivery, sensors, catalysis, and storage/separation (Furukawa & Yaghi, 2009; Hirscher & Panella, 2007; Snook et al., 2011).

As observed from recent research trends, MOFs and their hybridized nanostructures (e.g., metal oxides and porous carbons) have attracted attention in the development of electronic and electrochemical devices sensors, supercapacitors, solar cells, fuel cells, and Li ion batteries. Due to their very low intrinsic conductivities, the solitary use of MOFs for such applications is generally regarded as insufficient to obtain the desired results (Dey et al., 2012). Consequently, MOFs tend to be infused with other suitable materials to attain the desired levels of charge transport. Nonetheless, the introduction of conductivity to MOFs should not lead to a deterioration in their basic properties (e.g., high porosity and stability) (Mostaanzadeh et al., 2021)]. In this respect, it is noteworthy that the structures of MOFs can be modified in two different routes, either during their synthesis itself or through post-synthetic transformations. In the first approach, suitable materials are added during the synthesis of MOFs. This strategy provides an advantage that the added material undergoes superior bonding with either the metal component or the organic linker to help create more stable functional structures (Chen et al., 2017; Deep et al., 2015; Lee et al., 2015). Composite formation may also help in boosting the properties of individual components to induce synergistic effects on the overall performance. This technique can help reach the desired levels of conductivity while also maintaining the inherent characteristics of MOFs (Haque & Jhung, 2011; Kim et al., 2011).

Establishing a strong chemical bond between the carbon framework and MOFs would increase carbon accessibility for reactive species and enhance device performance (S. Xiong et al., 2020). MOFs with conductivities surpassing carbons have changed the perception of MOFs in energy storage devices due to the success of hybrid and conjugate structures. Energy storage applications have not yet fully utilized Fe-based MOFs (Flores et al., 2022; Sun et al., 2022).

Researchers developing Fe-MOF composite with carbon and mixed-valance metals, aiming to improve charge transfer and enhance electrode performance in SCs, surpassing carbon as a conduction electrode material, and Fe-MOF stands out for its highly conductive nature due to its lower effective nuclear charge and large radius. Due to their high surface area, adjustable pore sizes, and remarkable thermal and chemical stability, MOFs are suitable for applications and batteries. The iron-centered MIL MOFs facilitate redox reactions, improving their electrochemical properties (Chen et al., 2021; Ramasubramanian et al., 2022).

2.4.4. Transition metal oxides

Transition metal oxides are regarded as the next-generation electrode materials for ES applications due to their high specific capacitance, low cost, large voltage window, and low ESR In one words, transition metal oxide can provide higher energy density for ES than conventional capacitors and electrochemical stability than conductive polymers.

2.4.5. Metal oxide /Metal hydroxide

Metal oxides/hydroxides outperform conducting polymers and carbon materials in charge storage abilities, and specific capacitance. Supercapacitors with metal oxides/hydroxides electrode materials offer both high energy density and excellent power density (Pandolfo & Hollenkamp, 2006). Due to abundance of metal-based materials and the large number of synthesizable compounds, metal oxides/hydroxides are extensively researched in energy storage, particularly in the context of supercapacitors.

Electrochemical characteristics are influenced by it. Most metal oxides/hydroxides display pseudo-capacitive properties. Ruthenium oxide and manganese oxide are the most commonly studied materials for their high capabilities of storing several hundred farads over a broad potential window, achievable at high sweeping speeds. Most pseoudo-capacitive oxides function in aqueous electrolytes (Augustyn et al., 2014).

2.4.5.1. Nickel hydroxide

$Ni(OH)_2$ is hexagonal-layered structure and has two polymorphs, α- and β-$Ni(OH)_2$, corresponding to γ- and β-NiOOH after oxidizing (Yuan et al., 2021; J.-j. Zhang et al., 2020). α-$Ni(OH)_2$ is a hydroxyl-deficient phase with interlayered anions and water molecules. β-$Ni(OH)_2$ possesses a brucite structure without water molecules. α-$Ni(OH)_2$ /γ-NiOOH couple shows higher SC than β-$Ni(OH)_2$ /βNiOOH couple due to the greater change in valence. Under the common charging condition, $Ni(OH)_2$ transforms between β-$Ni(OH)_2$ and β-NiOOH. When the material is overcharged, β-NiOOH will change to γ-NiOOH and then α$Ni(OH)_2$ after discharging. α-$Ni(OH)_2$ is not very stable since it can transform to β-$Ni(OH)_2$ easily through aging in alkaline electrolyte (Bernard et al., 1996; Li et al., 2023; Ren et al., 2012).

The theoretical specific capacitance of $Ni(OH)_2$ is about 3650 F g^{-1} and its practical specific capacitance is much higher than NiO (Gurav et al., 2013; Jarvis et al., 2011). The powder materials usually show a specific capacitance s of 500−600 F g^{-1}, while the modified film can even reach an extremely high Cs of 3000 F g^{-1}, which is very close to the theoretical specific capacitance (Yu et al., 2020). The porous α-$Ni(OH)_2$ (Sugimoto, 2014) electrodeposited on Ni foam exhibits a very high SC of 3152 F g^{-1} at a current density of 4 A g^{-1}, but the specific capacitance drops quickly as the current density increases. The amazing specific capacitance can be attributed to its loosely crystal structure, which contributes to the easy insertion/extraction of ions and the hydratability of $Ni(OH)_2$ in favor of electrochemical reactions (Wang et al., 2018). The terrible rate capability due to the poor electric conductivity of $Ni(OH)_2$ and the poor cycle stability confine the application of $Ni(OH)_2$. The $Ni(OH)_2$ /carbon composites exhibit good rate capabilities and cycling performance. A Ni(OH) (Wang et al., 2011) /graphene sheet electrode demonstrates a high specific capacitance of 1335 F g^{-1} at a current density of 2.8 A g^{-1} and 953 F g^{-1} at 45.7 A g^{-1} with good rate capability, and there is no obvious capacitance drop at a current density of 28.6 A g^{-1}. The α-$Ni(OH)_2$ nanosheets composited with low defect density CNTs were fabricated by a one-step hydrothermal method. They delivered a higher specific capacitance of 1302.5 F g^{-1} than their components (372.1 F g^{-1} for $Ni(OH)_2$ and 101.4 F g^{-1} for carbon nanotubes), demonstrating the synergistic effects of the hybrid materials to enhance electrochemical performance.

2.5. Electrolytes

In supercapacitors, the electrolyte is a vital component that transfers and balances charge between the two electrodes (Xu, 2004). An electrolyte is an acid, base, or salt solution in a particular solvent. To achieve the charge storage phenomena, the electrolytes smooth the progress of the electrodes. Psedocapacitive capacitors have been used to conduct the reversible redox process, and electrolytes in ESs are crucial to the formation of EDL in EDLC. For any electrolyte, the most crucial elements are the ion concentration, size, type, and interaction with the electrode material (Iqbal et al., 2020). The condition of the electrode- electrolyte interface and the internal structure of active materials are greatly influenced by the interaction between the electrolyte and the electrode in all chemical processes.

Progress in designing electrolytes considering their electrochemical interaction with the electrode material in determining a supercapacitive device's performance indicators such as achievable capacitance (amount of charge stored), voltage window, charge storage time constants, characteristics, rate performance, cyclability, and safety have not been reviewed. The secret to high performance, safe supercapacitive devices is the selection of the electrolyte.

As of yet, no ideal electrolyte has been discovered that satisfies every need of an electrochemical device (B. Pal et al., 2019). The electrolytes for electrochemical supercapacitors are classified into various categories.

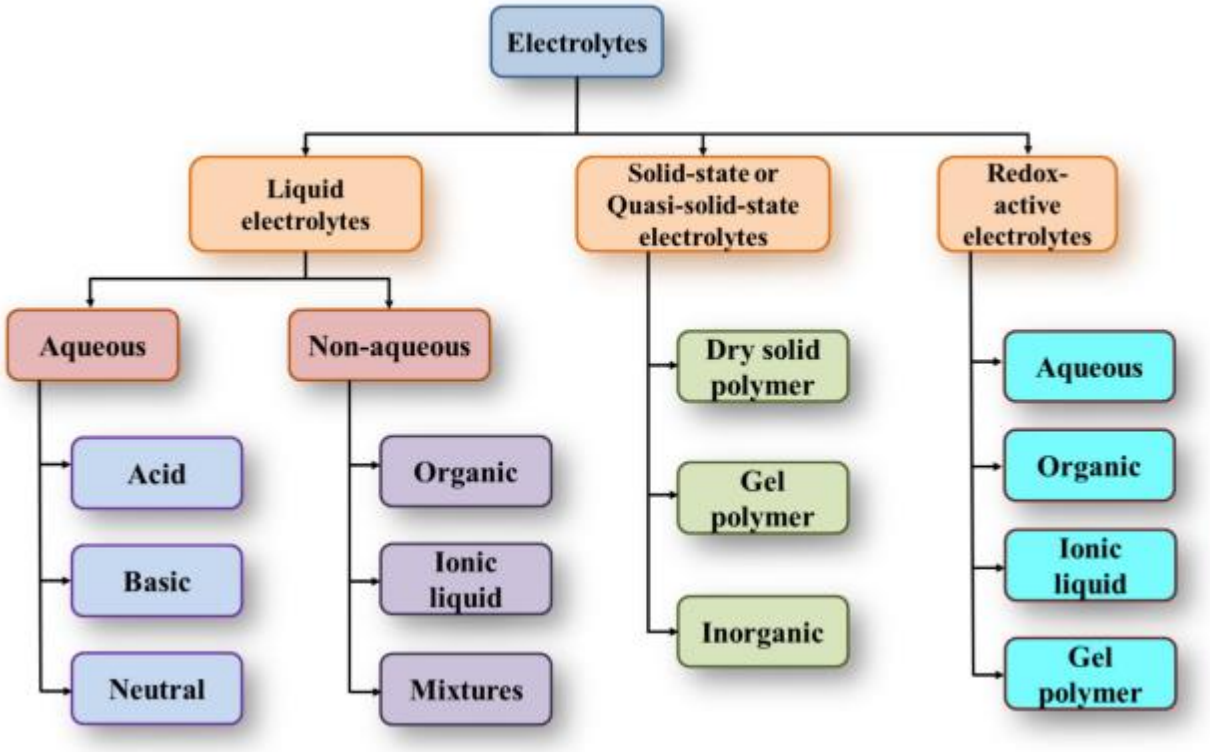

Figure 2. 7: classification of electrolyte for supercapacitor (Iqbal et al., 2020).

2.5.1. Aqueous electrolyte

Due to their ease of handling in the laboratory compared to organic electrolytes and ILS, which need purifying processes, aqueous electrolytes have been employed widely in research and development. Higher conductivity in aqueous electrolytes (Bhupender Pal et al., 2019) as opposed to organic and ionic electrolytes is advantageous for reducing the equivalent series resistance (ESR) and improving the power delivery of SC devices (Galiński et al., 2006).

Aqueous alkali- metal ion batteries can be made with materials whose potential is in the region between the evolution potential of O_2 and H_2. furthermore, as pH has a significant impact on the O_2 and H_2 evolution potentials of the aqueous system, attention should be taken while choosing the electrode materials (Kim et al., 2014).

Aqueous electrolytes are divided into three categories: (1) alkaline, (2) neutral, and (3) acidic solution. The most frequently used aqueous electrolytes are KOH (Iqbal et al., 2021), NaOH, LiOH, Na_2SO_4, H_2SO_4, $(NH_4)_2SO_4$, K_2SO_4, Li_2SO_4, and $MgSO_4$ among the aqueous electrolytes (Bhupender Pal et al., 2019).

Among the mostly used aqueous electrolytes KOH, NaOH, and Na_2SO_4 are some of them. The current response of these electrolytes decreases in the order of 6M KOH> 1M KOH > 1M NaOH > 1M Na_2SO_4. When compared to other electrolytes, KOH exhibits an improved current response. This is because the hydrated radius of K^+ ions is 3.31 Å, and Na^+ ions are 3.58 Å, respectively. The conductivity of K^+ ions (73 cm^2/Ω mol) was found to be higher at 25 ºC than that of Na^+ ions (50 cm^2/Ω mol) and Li^+ ions (38 cm^2/Ω mol). As a result, K^+ ions would have better ion mobility than Na^+ and Li^+ ions. Improved ionic mobility and contact with the electrode material are favored by the decreased hydrated radius of K^+ ions, which leads to improved electrochemical performance. The K^+ ions also acquire small charge density (weak salvation interactions with a water molecule that favors easier polarization during the de-salvation processes) which further helps K^+ ions go easily into the electrode during the redox reactions; concluding that the cations had a major role in the electrochemical reaction processes. To comprehend the function of anions in electrochemical performance, the CV results for Na_2SO_4 and NaOH electrolytes were compared. The redox peak was more prominent in the NaOH electrolyte as compared to the Na_2SO_4 electrolyte, according to the results (Nithya et al., 2013). This was because sulfate ions had a larger anionic size (1.49 Å) than hydroxyl ions (1.10 Å) (Bhupender Pal et al., 2019).

2.5.2. Organic electrolyte

For semiconductor devicess, organic electrolytes are usually conducting salt dissolved in organic solvents. Currently ruling the commercial market are devices based on organic electrolyte due to their high voltage window (2.6 to 2.9 V). Because of their larger molecules, which need larger hole size in the electrodes; organic electrolytes have a greater resistance than aqueous electrolytes. Just as with aqueous electrolyte- based SCDs, the characteristics of salt and solvents, including conductivity, viscosity, ion size, and ion- solvent interaction, have a significant impact on how well organic electrolyte- based SCDs works.

2.5.3. Ionic liquid electrolyte

Among the important parts of an SC device, a wise choice of electrolyte is vital to retaining the stability of the electrode materials at elevated temperatures. The organic electrolytes used in SCs at the commercial level are not suitable for temperatures above 70 °C because of their low ignition and detonation temperatures and aqueous electrolytes are limited by the boiling temperature of the water and cannot be used effectively above 80 °C. ILs are potential candidates for use at even very high temperatures because of their high chemical and thermal stabilities, with wide operating voltage ranges, negligible vapor pressure, and non-flammability (Raza et al., 2018).

2.6. Methods to synthesize electrode materials

2.6.1. Chemical method

There are two ways to make nanoparticles (NPs), including the top- down method, which involves starting with macro-sized materials and working down. In contrast, NPs are synthesized from atoms in the bottom-up technique. The bottom- up approach, which involves building NPs starting from atomic or molecular levels, assembles them into large particles successively, and simultaneously, is the more popular approaches between the two methods.

2.6.2. Co- precipitation method

Co-precipitation has been widely used to synthesize metal oxide-containing hybrids due to its simplicity and cost-effectiveness. proposed a straightforward, scalable, and cost-effective approach to synthesize high-performance supercapacitor electrode materials (Bae et al., 2019).

2.6.3. Hydrothermal

The hydrothermal method is one of the possible approaches to achieve the nanostructure among the synthesis techniques. The benefits of hydrothermal synthesis include ease of use, affordability, and eco-friendliness. Furthermore, the sample's morphology and structure can be easily adjusted by adjusting the temperature, time, and solution concentration (Chu et al., 2020; Hussain et al., 2024; Yadav & Sharma, 2021).

In their study,(Nidhi Tiwari, 2022) reported a facile and cost-effective hydrothermal route for the synthesis of $ZnFe_2O_4$ nanostructures on nickel foam using a binder-free approach. With a long-term cyclic stability of 1000 cycles, $ZnFe_2O_4$ delivered a superb specific capacitance of 552 F g^{-1} when used as an electrode for a high supercapacitor at a scan rate of 5mV/s. (Zhaojin Li, 2022) suggests a simple hydrothermal carbonization process to create 3D hierarchical ordered porous carbon doped with O-N. The hierarchical-ordered porous carbon displayed a super high specific surface area of 1952 m 2 g^{-1} and outstanding conductivity. At a current density of 0.5 Ag^{-1}, the carbon material displayed an exceptional gravimetric capacitance of 556.0 F g^{-1} (Zhaojin Li, 2022). Based on the CV test, 5mV/s. Ce-doped Co_3O_4 nanoflakes exhibited great specific capacitance of 1309.6 F g^{-1} and high cyclic stability of 90.86% after the 2000 CV cycle at a scan rate of 5mv/s. The GCD test at 1-10 Ag^{-1} demonstrated high current density of 10A g^{-1} indicating excellent rate of capability (Ali et al., 2021). Nikel tungstate nanostructure with pronounced supercapacitor and electrochemical sensing activities was synthesized using the hydrothermal method. Specific capacitance of 1524 F g^{-1} at a current density of 0.5 Ag^{-1} was reported. At a power density of 2206 Wkg^{-1} a maximum current density of 32.27 $WhKg^{-1}$. Furthermore, large charge/discharge time as 1353s, corresponding to the current density of 0.5 Ag^{-1} has been stated (Muhammad Ikram, 2021).

2.6.4. Electrodeposition

The electrochemical deposition of MOFs, with its mild preparation conditions, continuous process monitoring, controllable synthesis parameters and potential for large-scale production, is a newly emerging method in comparison to others. Now the focus on MOF films electrochemical deposition is shifting from preparation to application(Sun et al., 2021; X. Zhang et al., 2020). The thickness of the deposited film is controlled by varying the electrode potential and current density(Kale et al., 2021).

In the study by (M. Zhang et al., 2020) high quality MnO_2 nano dendrites were electrodeposited on three-dimensional porous nickel foam. At 0.6 V depositions potential and 1 Ag^{-1} current density, the specific capacitance reached 469 Fg^{-1}. Moreover, after 2500 cycles, capacity retention was 83.9%, and the specific capacitance maintained at about 358 Fg^{-1} at a high current density of 5 Ag^{-1}. At a specific power of 2544W Kg^{-1}, it reached specific energy of 50.52 Wh Kg^{-1}. In other work, a facile electrodeposition method was used to fabricate a suite of coral-like

nickel cobalt hudroxysulfied nanosheet arrays (NiCo-SOH) on nickel foam (NF), which was expected to be a binder-free positive electrode for supercapacitors. An excellent specific capacitance and superior rate capability (2092.7 Fg^{-1} at $1Ag^{-1}$; $1696Fg^{-1}$ at 10 Ag^{-1}) Moreover, a NiCo-SOH (Ni:Co1:1) electrode and active carbon (AC) were used to fabricate an asymmetric supercapacitor, which showed a high cyclic stability (98% capacitance retention after 9000 cycle) and excellent energy density of 34.3 Wh Kg^{-1} (Pu et al., 2021).

Furthermore, MSCs with large areal specific capacitance of $719.2mFcm^{-2}$ at a current density of $0.5mAcm^{-2}$, which is almost 370 times higher than that of Micro supercapacitors prepared by laser-induce graphene were fabricated through the layer-by-layer (LBL) electrodeposition of porous polyaniline and MOF. The prepared MSCs retained more than 87.6% of their capacitances after 6000 cycles of charge-discharging test, showing their promising cyclic stability (Wang et al., 2020). The Ce/Ni-MOFs electrode material prepared by one-step electrochemical deposition avoids adhesives. Moreover, the flexible supercapacitor assembled based on Ce/Ni-MOFs//GO achieved a high voltage of 1.7V and showed remarkable capacitance ($298.8mFcm^{-2}$), excellent energy density (120.1 μWh cm^{-2}) and good durability (93% after 5000 cycles) (Liu et al., 2023).

CHAPTER THREE

3. MATERIALS AND METHODS

3.1. Chemicals and Materials

All of the chemicals reagents were of analytic grade: PET waste was obtained from water bottles, Iron sulfate heptahydrate ($FeSO_4.7H_2O$) was purchased from LOBA CHEMIE PVT.LTD(India), Nickel nitrate hexahydrate ($Ni(NO_3)_26H_2O$) (loba chem. 98% purity, India), Methanol(95% purity), dimethylformamide (DMF,99%) Ethanol, NaOH (97 % Mumbai, India), hydrochloric acid (HCl) and distilled water (DW) was used throughout the experiment.

3.2. Experimental Design

3.2.1. Synthesis of Terephthalic Acid

The synthesis of terephthalic acid (TPA) was carried out with little modification (Cosimbescu et al., 2021). PET bottles were gathered from Adama Science and Technology University garbage. then the bottle was carefully cleaned with water and dried at 60ºC for 30 min. After it dried 5 g of PET chips (1 x 1 cm) were cut out of PET bottle and were hydrolyzed in methanol (100ml) with 25g of NaOH and boiled for 4 hours at 80 ºC in a closed beaker at with continuous stirring. The solution cooled to room temperature and 250 ml distilled water was poured into the solution. The solution was filtered with a filter paper if there were undissolved PET chips then it was acidified with hydrochloric acid (6N) until the pH became 3. The precipitate was stirred for an additional 10 minutes. Then centrifuged at 500 rpm to separate the precipitate and to get rid of unwanted materials. Finally, the product was dried at 100 ºC for 12 hours.

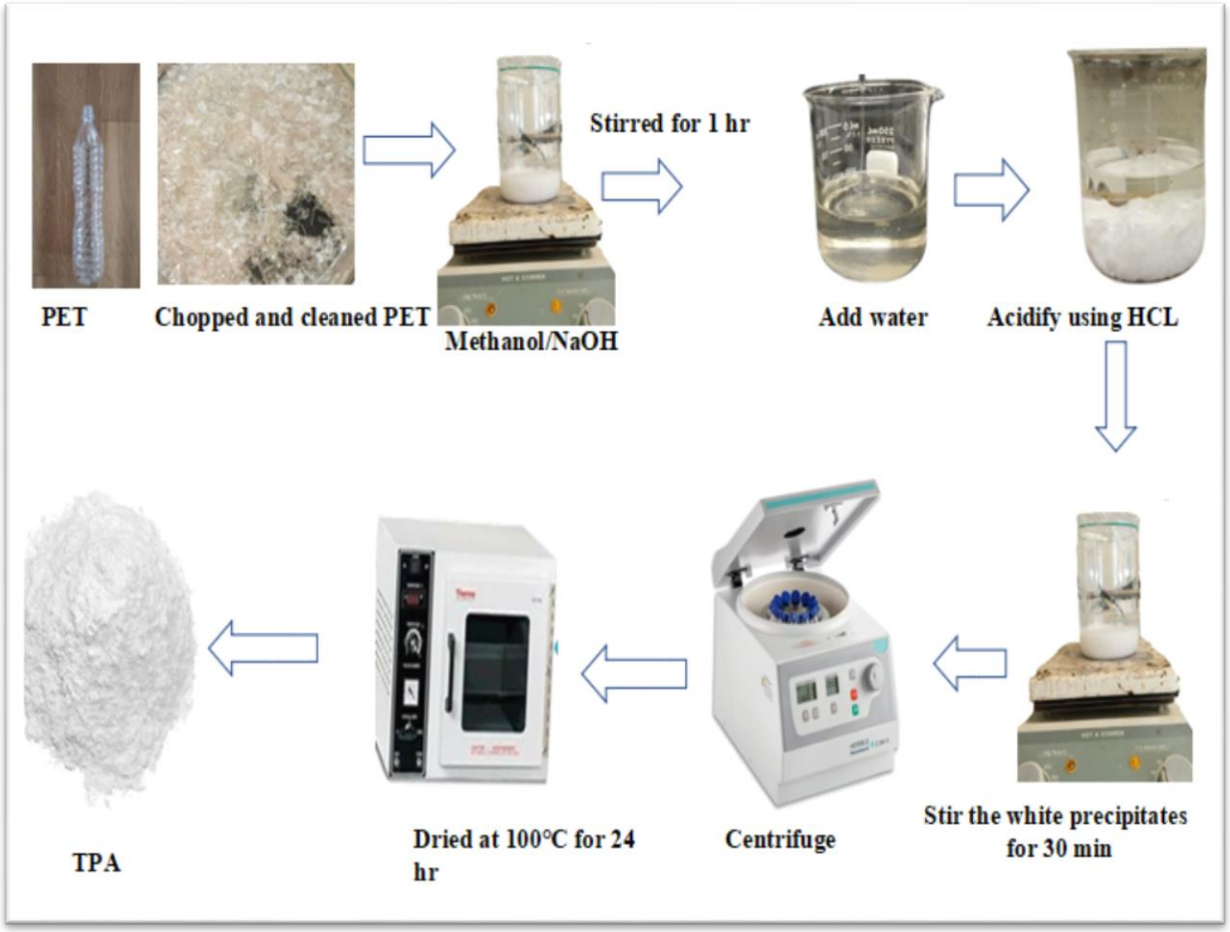

Figure 3. 1: Schematic illustration of the TPA formation process.

3.2.2. Synthesis of MIL-53(Fe)

The MIL-53(Fe) was prepared following a modified method (Lee et al., 2022).An equivalent amount of terephthalic acid (6 mmol) and iron sulfate heptahydrate(6mmol) was dissolved in 30 ml of DMF. Then solution was then sonicated for 1 hour each then the terephthalic acid solution was added into the iron solution then continuously sonicated for 1 hours at 70ºC. Then stirred for 6hr at 100ºc , was washed with ethanol. Finally, the product was dried at 120 ºCfor3hrs.

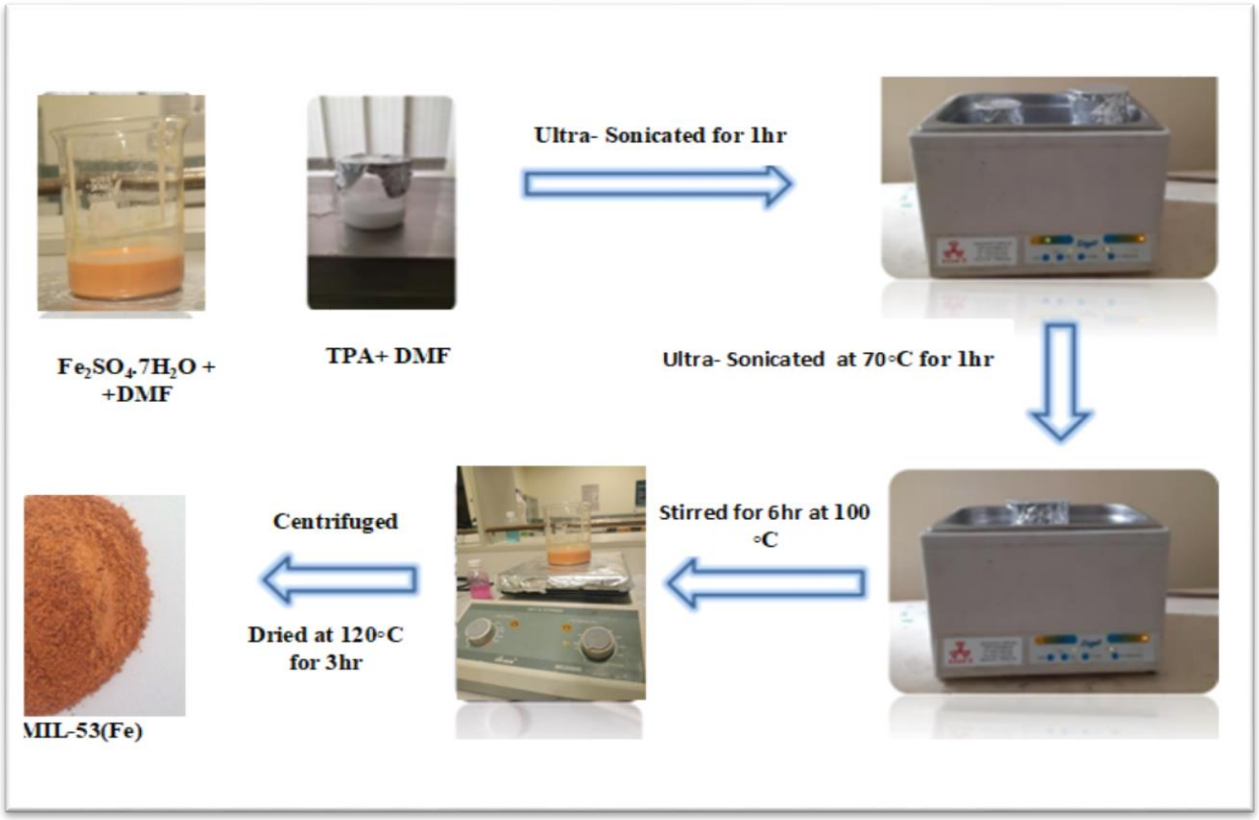

Figure 3. 2: Schematic illustration of the MILL-53(Fe) formation process.

3.2.3. Synthesis of β-Ni(OH) $_2$

β-Ni(OH)$_2$ was prepared as the reported with little modification (Mohanraj et al., 2024). In the specific procedure, 100ml of distilled water were used to dissolve 0.3M (100 ml) of Nickel nitrate hexahydrate for 30 minutes, and then 0.1M of NaOH was used to maintain the PH at 10 while being continuously stirred for two hours at 60ºC. The solution was aged for 10 hours and precipitates repeatedly rinsed with distilled water, centrifuged for 10 minutes at 1200 rpm, and dried in an oven at 100 ºC for 12 hr .

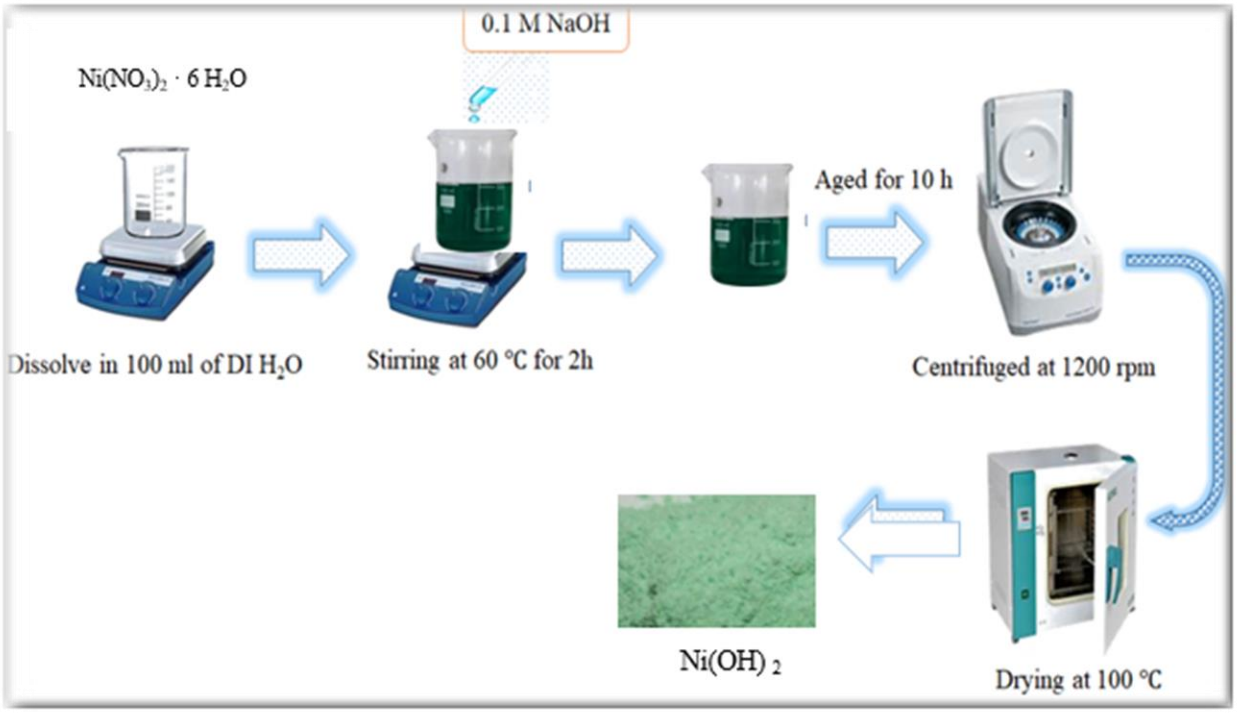

Figure 3. 3: Schematic illustration of the β-Ni(OH)$_2$ formation process.

3.2.4. Synthesis of MIL-53(Fe) /Ni $(OH)_2$

A wet chemical ultrasonic assisted synthesis process was used to make the MIL-53(Fe) /Ni $(OH)_2$ composite (figure 3.4) . Typically the different weight ratios of β-Ni$(OH)_2$ were added to MIL-53(Fe) in 30 ml ethanol solution, namely 10%, 20%, and 30%. The mixed solution was ultrasonically treated for 30 minutes and stirred for 2 hours. The obtained solid was then dried for 6 hr at 100ºC.

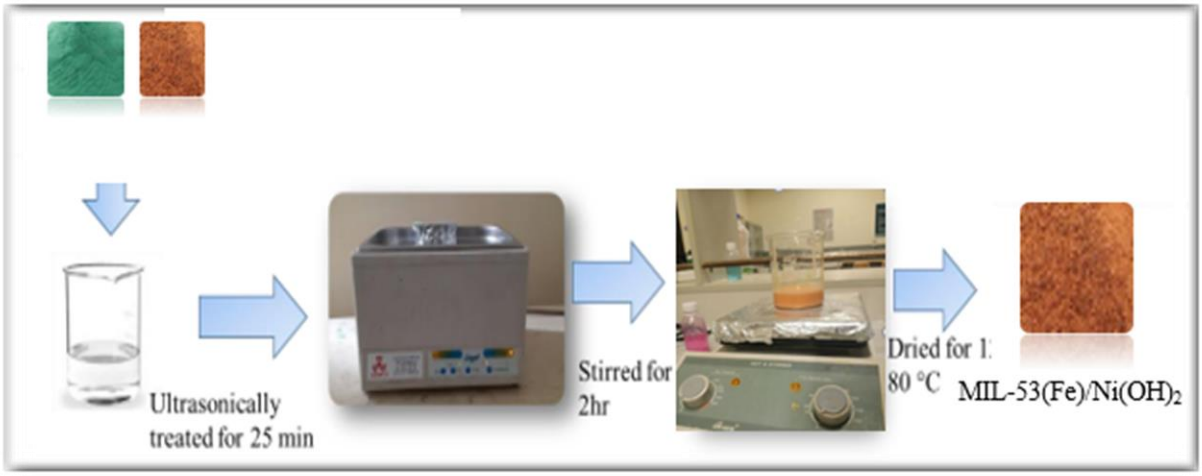

Figure 3. 4: Schematic illustration of the MIL-53(Fe)/Ni(OH)2 formation process.

3.3. Characterization

X-ray powder Diffraction (XRD) (Shimadzu XRD-7000) characterized the crystallinity, crystalline size, and phase of the catalysts. Fourier Transform Infrared Spectroscopy (FTIR) with Spectrum (NicoletTMiS50) was performed using KBr pellets for the chemical functional group analysis. Scanning Electron Microscopy (SEM) using JSM 6500F JEOL was used for Morphology, analysis.

3.3.1. Electrochemical characterization

3.3.1.1. Electrochemical test

The Biologic SP300 potentiostat electrochemical workstation (Won-A-Tech Co. Ltd, South Korea) was used for voltammetric measurements. A standard three-electrode cell was used, for voltammetric measurements. A standard three-electrode cell was used, with the as-prepared electrode (GC, MIL-53(Fe)/GC, $Ni(OH)_2$ /GC, M-Ni1, M-Ni2, M-Ni3 serving as working electrode, and Ag/AgCl as the reference electrode in aqueous electrolyte and platinum wire as a counter electrode.

3.3.1.2. Electrode preparation

The glassy carbon GC50 with a disk diameter of 3 mm was used as a working electrode. The active area of glassy carbon was cleaned by polishing it using alumina powder and emery paper until it looked like a mirror. The alumina fine powder and emery paper were used for that purpose. Finally, it was washed with deionized water and acetone (Gamil et al., 2019).The slurry was prepared by dispersing a mixture of active material (MIL-53(Fe)/$Ni(OH)_2$), reduced graphene oxide, and nafion with a weight ratio of (80:10:10). Thereafter, the mixture was sonicated for 10 min and 50 μL of the obtained slurry was drop-casted over the active area and dried at room temperature for 5 hours.

Figure 3.5: Schematic representation of glassy carbon working electrode used.

3.3.1.3. Cyclic Voltammetry

Cyclic voltammetry (CV) is the most useful electrochemical technique, which can provide the kinetics, and thermodynamics information related to the redox reactions within a system. Moreover, it also enables to investigation of thoroughly diverse characteristics, the number of electrons carried over in charge transfer reaction, the adsorption during the cyclic voltammetry (CV) test, the potential is applied, and the current is measured. Therefore, the CV curve represents a function of the measured current versus the applied potential.

Previous studies have demonstrated that the charge storage capacity and the specific capacitance of a supercapacitor electrode could be calculated using the cyclic voltammetric (CV) curves through equation](Wei Chen et al., 2010; Hu & Tsou, 2002).

$$Specific\ capacitance = \frac{voltammetric\ charge}{potntial\ window\ X\ active\ material\ mass\ loading} \text{-----} (3.\ 1)$$

3.3.1.4. Galvanostatic charge-discharge

Galvanostatic charge/discharge (GCD) is a traditional method to evaluate a series of SC performance parameters, such as capacitance, energy density, power density, ESR, and cycle stability. The GCD process follows the responsive potential relative to time and calculates information associated with an electrochemical phenomenon's occurrence in the SC electrode material. The overall GCD measurement process involves two steps: first, the SC charges via a constant current, and second, it is discharged in a specific time or voltage range. The capacitance can be estimated using Equation 3.2:

$$Specific\ Capacitance\ (Cs) = \frac{i\Delta t}{\Delta V} \text{---------- } (3.\ 2)$$

Where i denotes the discharging current, ΔV is the discharge voltage for a device, and Δt is the discharging time (Areir et al., 2017; R. Zhang et al., 2015). The single-electrode specific capacitance (Cs) can be obtained.

$$Cs = \frac{i\Delta t}{A\Delta V} \text{---------- } (3.\ 3)$$

Where i is again the discharging current, ΔV is the discharge voltage for a device, A denotes the total area of two electrodes, and Δt can be one of several attributes, such as the discharging time (Li et al., 2017; Ma et al., 2018).

In this study the specific capacitance of the potential electrode material was calculated using the CV and GCD using galvanometric and areal capacitance respectively.

3.3.1.5. Electrochemical Impedance Spectroscopy

The electrochemical impedance spectroscopy (EIS) is a critical investigation technique used to investigate the electrochemical phenomenon at the electrode-electrolyte interface. The EIS data collection consists of the application of a sinusoidal potential by a small amplitude in a wide range of frequencies from 100 kHz to a few MHz to a regular state. Generally, the Electrochemical impedance spectroscopy (EIS) data is presented by a curve of –Im(Z) versus Re(Z) which is known as the Nyquist plot where: Re(Z) is the real part of the impedance and Im(Z) : is the imaginary part of the impedance.

CHAPTER FOUR

4. RESULTS AND DISCUSSION

4.1. X-Ray Powder Diffraction (XRD) Analysis

The crystal structure and purity of the prepared sample were determined by power XRD analysis. Figure 4.1 a) displays a typical XRD pattern of as-prepared TPA which exhibits various well-defined diffraction peaks appear at 2Ɵ =17.30 º, 25.13 º, 27.85 º, 29.58 º, and 39.57 º. The observed diffraction peaks are well consistent with the reported literature, which confirms the successful formation of TPA (Cosimbescu et al., 2021), and Figure 4.1 b) shows XRD patterns of the synthesized samples of MIL-53(Fe) shows well-defined peaks at various angels corresponding to specific plans in the crystal structured. The observed peaks are 9.24º, 11.7º, 17.66º, 18.24º, 18.58º, 25.52º, 27.32º, 29.8º, 30.28º are in good agreement or almost the same with the reported pattern [CCDC NO. 690316] (Millange et al., 2008). However, there was a small variation in some of the peaks due to the flexible nature of MIL-53(Fe) (Asghar et al., 2024; Walton et al., 2011). Figure 4.1 c) is the XRD patterns of β-$Ni(OH)_2$ eight diffraction peaks. In Figure 4.1 c) (2Ɵ=19.5º, 33.4º, 38.8 º, 52.5º, 59.3º, 70.9º and 72.7º) were attributed to (001), (100), (101), (102),(110),(111), (103), and (201) diffraction of β- $NI(OH)_2$ (JCPD Card No. 059-0463), respectively, which indicates that both products obtained are β- $NI(OH)_2$ phase. The XRD pattern of MIL-53(Fe)/$Ni(OH)_2$ shows that following the entrance of $Ni(OH)_2$ to the system, at 2θ peaks of 19.5˚, 33.4˚,38.8˚,59.3˚ and the remains peak unchanged.

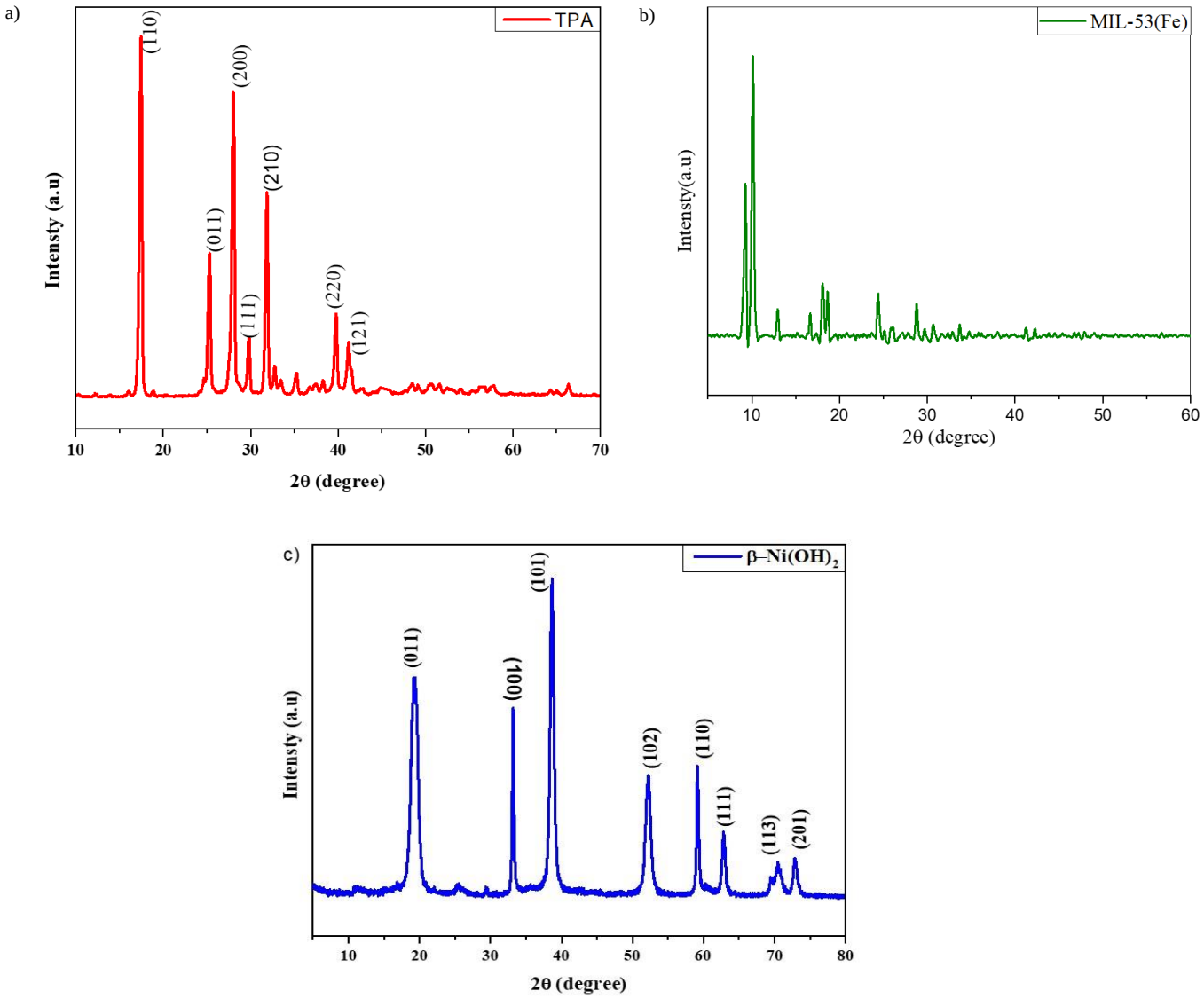

Figure 4. 1: XRD of a) TPA b) MIL-53(Fe) c) β-Ni(OH)$_2$

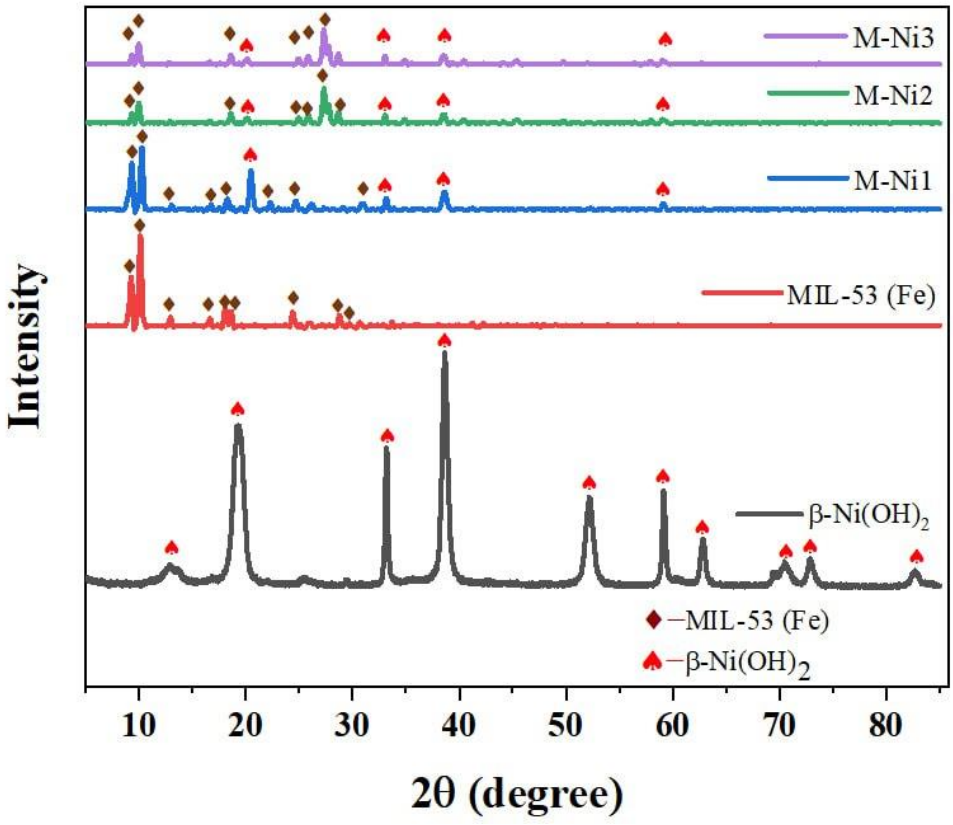

Figure 4. 2: XRD of MIL-53(Fe)/Ni(OH)₂

4.2. Fourier Transform Infrared Spectroscopy (FTIR) Analysis

The FTIR analysis of the as-prepared samples was carried out in the skeletal region of 500-4000 cm^{-1}. **Figure (a-b)**, shows the results of the FTIR spectra of TPA, MIL-53(Fe), β-$Ni(OH)_2$, MIL-53(Fe)/$Ni(OH)_2$ materials were analyzed at room temperature to determine the chemical bond present in each sample.

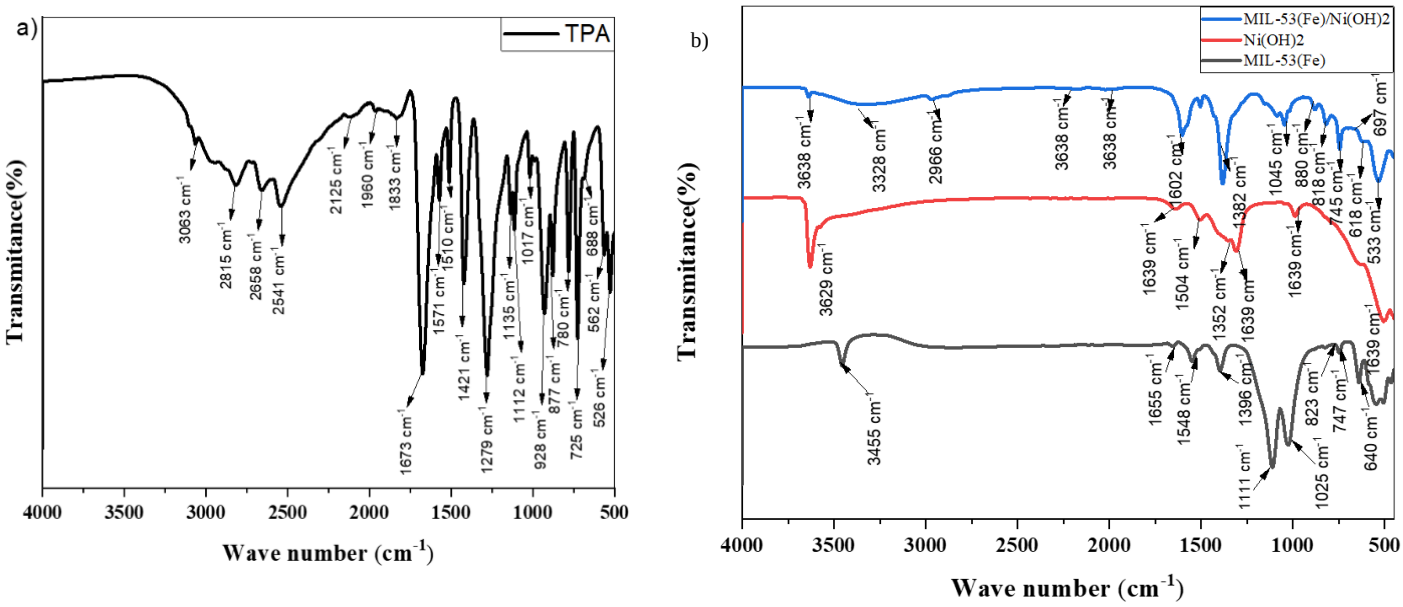

Figure 4. 3: FTIR spectra a) TPA b) MIL-53(Fe), β-Ni(OH)$_2$,MIL-53(Fe)/β-Ni(OH)$_2$

In the FTIR spectrum of TPA, figure 4.2 a) the characteristic peaks were observed between 2541 cm^{-1} and 3100 cm $^{-1}$ and 446-1571 cm^{-1}. The peak between 2541 cm^{-1} and 3100cm^{-1} are related to the –COOH stretching vibration. While the peaks at 1673 cm-1 are related the -C- stretching vibration from aromatic ring. The peaks observed in the region 1421-1572 cm^{-1} are related to the C-C stretching vibration from the aromatic ring. Moreover, the peaks observed in the region 928-1279 cm^{-1} are assigned to –C-OH, -C-CH, and –C-H groups present in the TPA, The characteristic peaks corresponding to aromatic ranges were observed at 700-800 cm^{-1}.

To identify the functional groups of the MIL-53 (Fe) sample, FTIR spectroscopy was performed and the result is shown in figure 4.2 b) the characteristic absorption peaks of the MIL-53(Fe) sample appear at 1680,1548,1396,1025, and 747 cm^{-1}, which could mainly originate from the carboxylat groups vibration and are identical to those of reports (Nivetha et al., 2019) the broad peak centered at 3445 cm^{-1} is associated with the starching vibration of O-H from the surface adsorbed water.

The two sharp peaks at 1548 and 139 cm^{-1} are assigned to asymmetric (Vas(C-O)) and symmetric (Vas(C-O)) vibration of carboxyl groups, respectively, confirming the presence of a dicarboxylate linker within the sample. The peaks at 750 cm^{-1} corresponding to the C-H bending vibrations of benzene. The intense peak at 3455 cm^{-1} is related to the Fe-OH vibrations.

The quality and composition of the as-prepared β-$Ni(OH)_2$ were examined by FTIR spectroscopy in the range of 400-4000cm^{-1}. The results are shown in figure 4.3 b) FTIR spectrum verifies that the prepared $Ni(OH)_2$ can characterized as β form, due to the existence of a narrow and strong band at 3629 cm^{-1} relating to the v(OH) stretching vibration, which indicates OH groups in a free configuration, and The broad and intense band centered at 3448 cm^{-1} is assigned to the O-H stretching vibration of the interlayer water molecules and of the H-bound OH group. Also, another peak observed at 1639 cm^{-1} is assigned to the bending vibration of water molecules. The peaks located between 800-1800cm^{-1} could be assigned to the presence of anions, which have probably not been completely eliminated during the washing stage. The peak observed at 1540cm^{-1} is transferred to the vibration mode of the carbonated groups originating from the adsorption of atmosphere CO_2.

The FTIR analysis of the M-Ni-20% composite confirms the effective formation of the MIL-53(Fe)/ $Ni(OH)_2$ composite. The result showed that the characteristics bands related to the functional groups of MIL-53(Fe), β-$Ni(OH)_2$.

4.3. Brunauer, Emmett, and Teller (BET) Analysis

Table 1: : the measured BET data of β-Ni(OH, MIL-53(Fe),and M-Ni2 nanoparticles

	Bare-β-Ni(OH)2	MIL-53(Fe)	M-Ni2
Specific surface area (a_s)	503.159 m^2/g	557.151 m^2/g	598.681 m^2/g
Total pore volume	0.1008 m^3/g	0.7100 m^3/g	0.9310 m^3/g
Pore size	0.12 (nm)	0.69 (nm)	0.88 (nm)

Brunauer, Emmett, and Teller (BET) analysis is a technique used to measure the surface area of materials. The specific surface area of the M-Ni2 powder was 598.681 m^2/g, compared to 503.159 m^2 /g for the bare $Ni(OH)_2$. When $Ni(OH)_2$ nanoparticles are encapsulated by MIL-53(Fe), the surface area of the composite increases. Mil-53(Fe) have high porosity and act as a encapsulating agent, which decreases the formation of agglomeration and increase the active cite in MIL-53(Fe)/$Ni(OH)_2$ composite at optimal concentration, the surface area of the M-Ni2 composite increased compared to the other concentrations. These designs allow the electrode material to come into contact with the electrolyte, which can increase the overall capacitance of the SC.

4.4. Scanning Electron Microscope (SEM) Analysis

Scanning electron microscopy (SEM) was used to study the surface morphology of pure β-$Ni(OH)_2$, MIL-53(Fe), and M-Ni2 nanoparticles. The image in figure shows that the first β-$Ni(OH)_2$ image has a typical flat, sheet-like structure with less porosity. On the other hand, MIL-53(Fe) exhibits an porous material as observed from the BET analysis and interconnected structure loosely agglomerated (Liu et al., 2015). The SEM image of the 20% β-$Ni(OH)_2$ impregnated composite reveals a connected structure with porosity, but no flat sheet-like structure at the surface is observed on the surface. This suggested that the $Ni(OH)_2$ is impregnated within the MIL-53(Fe) structure (Pan et al., 2023; Zhu et al., 2023).

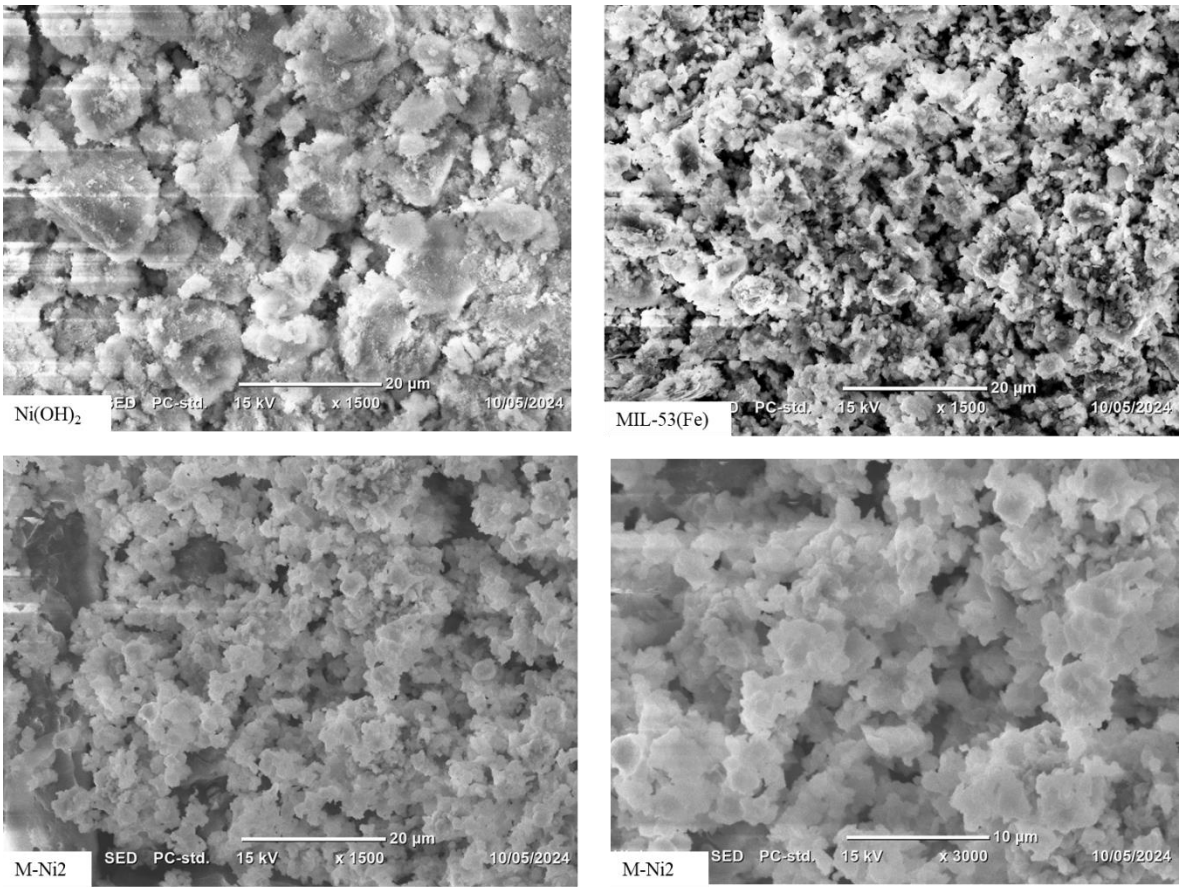

Figure 4. 4: SEM image of MIL-53(Fe), β-$Ni(OH)_2$ and M-Ni 20%

4.5. Electrochemical Characterization

In the current study, 1M Na_2SO_4 aqueous electrolytes were used to evaluate the electrochemical behavior of MIL-53(Fe)/$Ni(OH)_2$. The CV curves were collected in a voltage range from 0-0.6 V at various voltage sweeps 5, 10, 20, 40, 60, 100,150, and 200 mV/s. in addition, galvanostatic charge- discharge(GCD) using chronopotentiometry (CP) were measured. The electrochemical impedance spectroscopy (EIS) measurements were performed with an AC amplitude of 5mV in the frequency range of 100 kHz to 10mHz.

4.5.1. Cyclic voltammetry

Cyclic voltammetry (CV) measurements were carried out via a three-electrode setup across varying scan rates, ranging from 5mV/s to 200 mV/s. figure 4.5 display. $Ni(OH)_2$ electrode material exhibits the ideal capacitive behavior (Wenguo Chen et al., 2010; Sichumsaeng et al., 2018). A nearly rectangular shape CV graph at a different scan rate and a potential window ranging from 0 to 6V.

The limited potential window is a result of water's inherent electrochemical stability. Water can be decomposing at relatively low voltages, leading to the production of hydrogen and oxygen gases through electrolysis. Water oxidizes to oxygen at approximately +1.23 V compared to the standard hydrogen electrode (SHE), while it reduces to hydrogen at around -0.83 V versus SHE. As a result, the potential window for aqueous electrolyte is typically restricted to about 1.23 V. If the voltage exceeds this range, the efficiency of the electrochemical device decreases, and an increased risk of gas evolution and potential corrosion of the electrodes (Kim et al., 2014; B. Pal et al., 2019).

a)

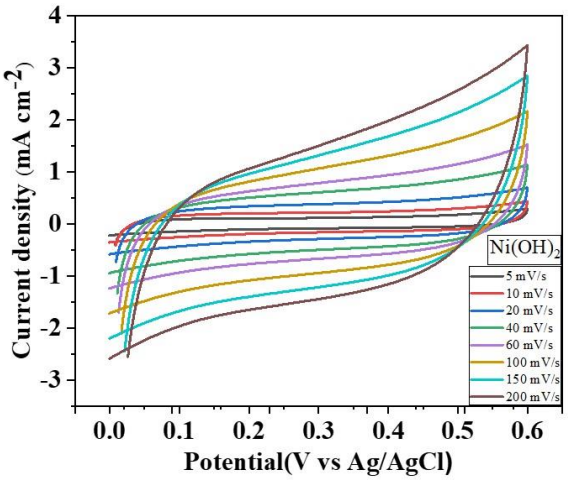

b)

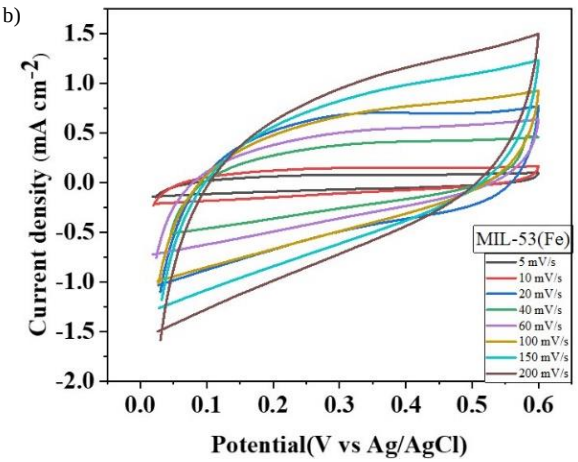

Figure 4. 5: CV curve of $Ni(OH)_2$ and MIL-53(Fe) electrodes at different scan rates

The effect of the electrolyte and the type of material used either its EDLs or Psudocapactor influence the shape of the CV graph, which is a nearly rectangular shape that has a pseudo-capacitance nature of the materials (Lu et al., 2013; Patra et al., 2021).

In the psedocapacitor it will be a redox reactions that will result in CV materials like $Ni(OH)_2$ exhibit a distorted rectangular- like shape main energy storage mechanism of ion adsorption and redox reaction which is one of the underpotential pseudocapacitor reaction is due to the adsorption and desorption of ions at the electrode surface (Patra et al., 2021).

Figure 4.5 displays the CV of the MIL-53(Fe) at different scan rates. With an increase in scan rate, the recorded current density increases accordingly (Li et al., 2012). However, the reductions in capacitance values were attributed to surface pore diffusion restrictions as the scan rate increased (El-Shahat et al., 2020).

To further explore the influence of different β- $Ni(OH)_2$ loading on the electrochemical performance of MIL-53(Fe)@ $Ni(OH)_2$ materials, the CV was conducted at a different scan rate between 5mV/s to 200mV/s on M-Ni, M-Ni1, M-Ni2, ML-Ni3 are shown in figure 4.6**.**

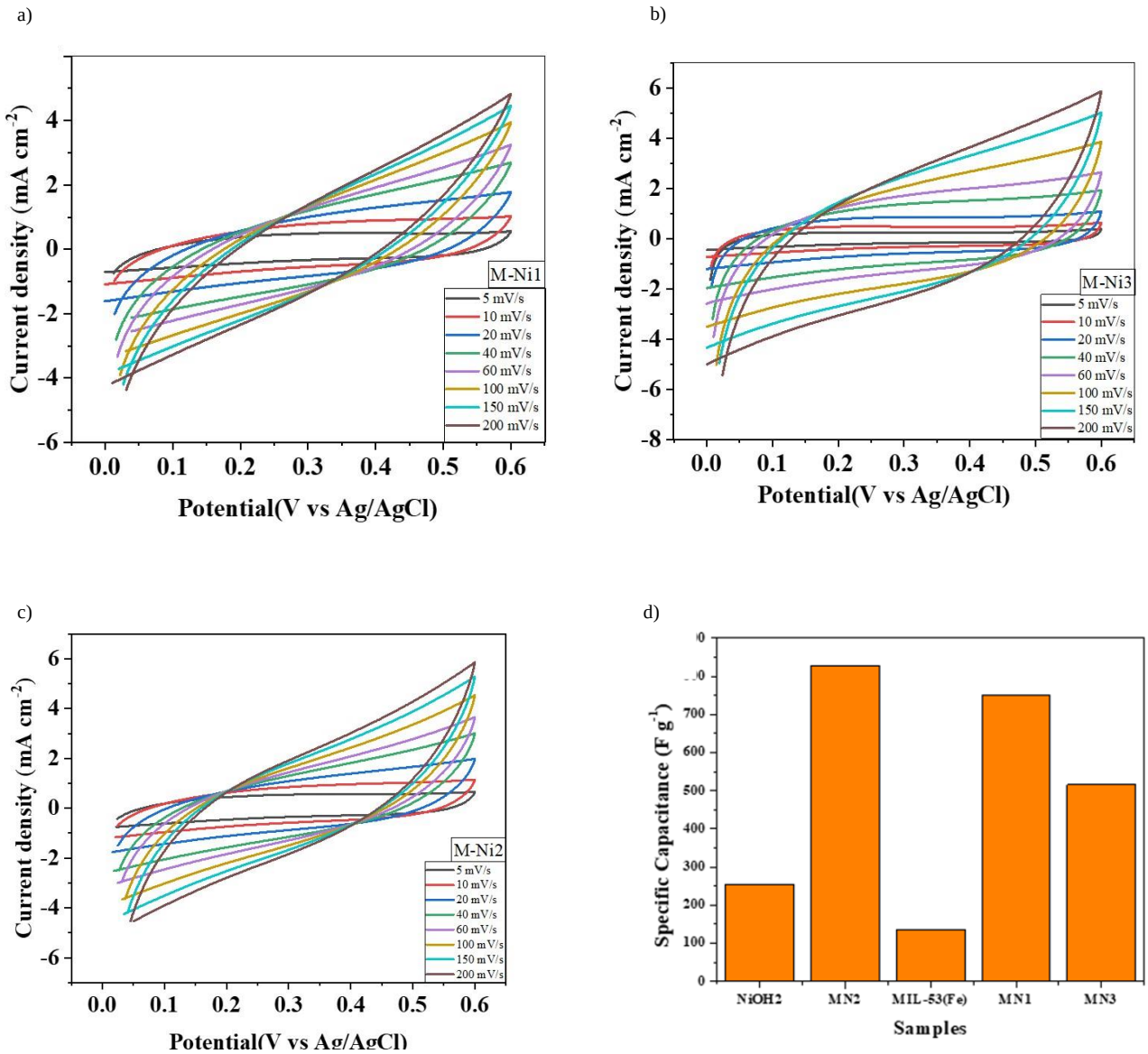

Figure 4. 6: a-c) CV curve of M-Ni1, M-Ni2, M-Ni3 electrodes at different scan rate. b). Specific capacitance calculated using CV at different concentration.

Table 2:specific capacitance calculated using CV at different concentration

Scan rate	Cp of MIL-53(Fe)	Cp of Ni(OH)2	Cp of MN1	Cp of MN2	Cp of MN3
10mV/s	136.6F/g	254.166 F/g	750 F/g	828.33 F/g	515 F/g

The amount of $Ni(OH)_2$ loading cannot fully embody the MIL-53(Fe) structure which influences the performance of MIL-53(Fe)@ $Ni(OH)_2$, so selecting the appropriate loading amount of $Ni(OH)_2$ play an important role in the electrochemical characteristics of the designed MIL-53(Fe)@ $Ni(OH)_2$ electrode material. Figure 4.6 d) shows the specific capacitance of bare and different concentration electrode materials at a fixed scan rate of 10mV/s. The M-Ni2 concentration shows the highest specific galvanometric capacitance, that is 828.33 F/g as in table 1. This is due to the amount of perfect loading of $Ni(OH)_2$ which influences the porosity to transport ions and also the synergetic effect between them is one of the reasons to achieve the specific capacitance among the other concentrations.

4.5.2. Galvanostatic charge/discharge (GCD)

Galvanostatic charge/discharge (GCD) is evaluates a series of SC performance parameters, such as capacitance, cycle stability using Chronopotentiometry technique (CP). In order to determine information's related to an electrochemical phenomenon occurring in the SC electrode material, the GCD process tracks the responsive potential in relation to time. Two steps make up the entire GCD measuring process: the SC is charged with a constant current in the first step, and it is discharged within a predetermined voltage range or time.

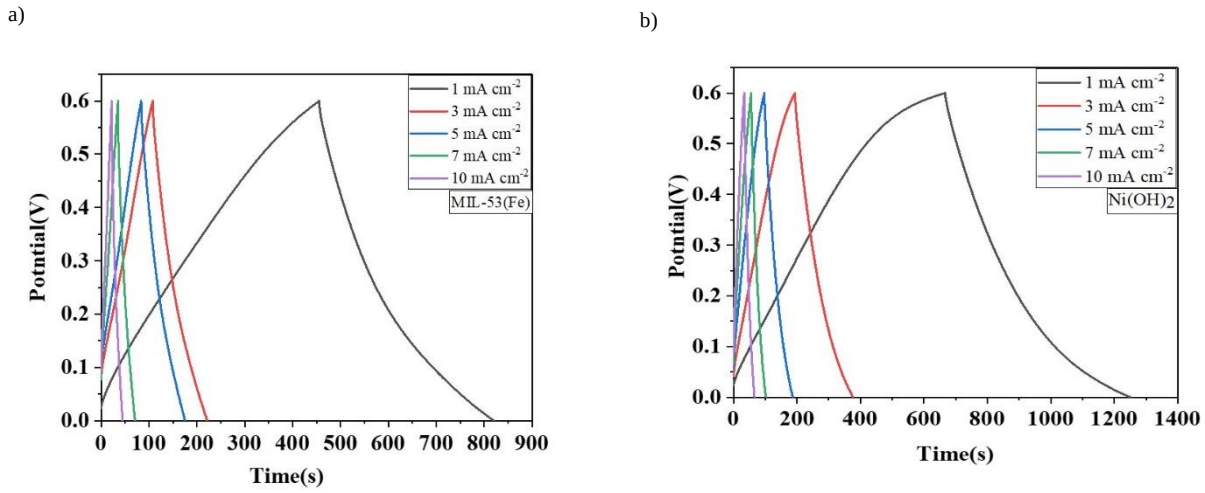

Figure 4. 7: a) GCD curve of MIL-53(Fe) at a different current density b) Ni(OH)2 at a different current density

The charge- discharge electrochemical performance of MIL-53(Fe), $Ni(OH)_2$, and their composite MIL-53(Fe)/$Ni(OH)_2$ at different concentration of $Ni(OH)_2$ was investigated at various current density of 1mA/cm^2, 3mA/cm^2, 5mA/cm^2, 7mA/cm^2,10 mA/cm^2. In Figure 4.6 shows the charge- discharge of MIL-53 and $Ni(OH)_2$.

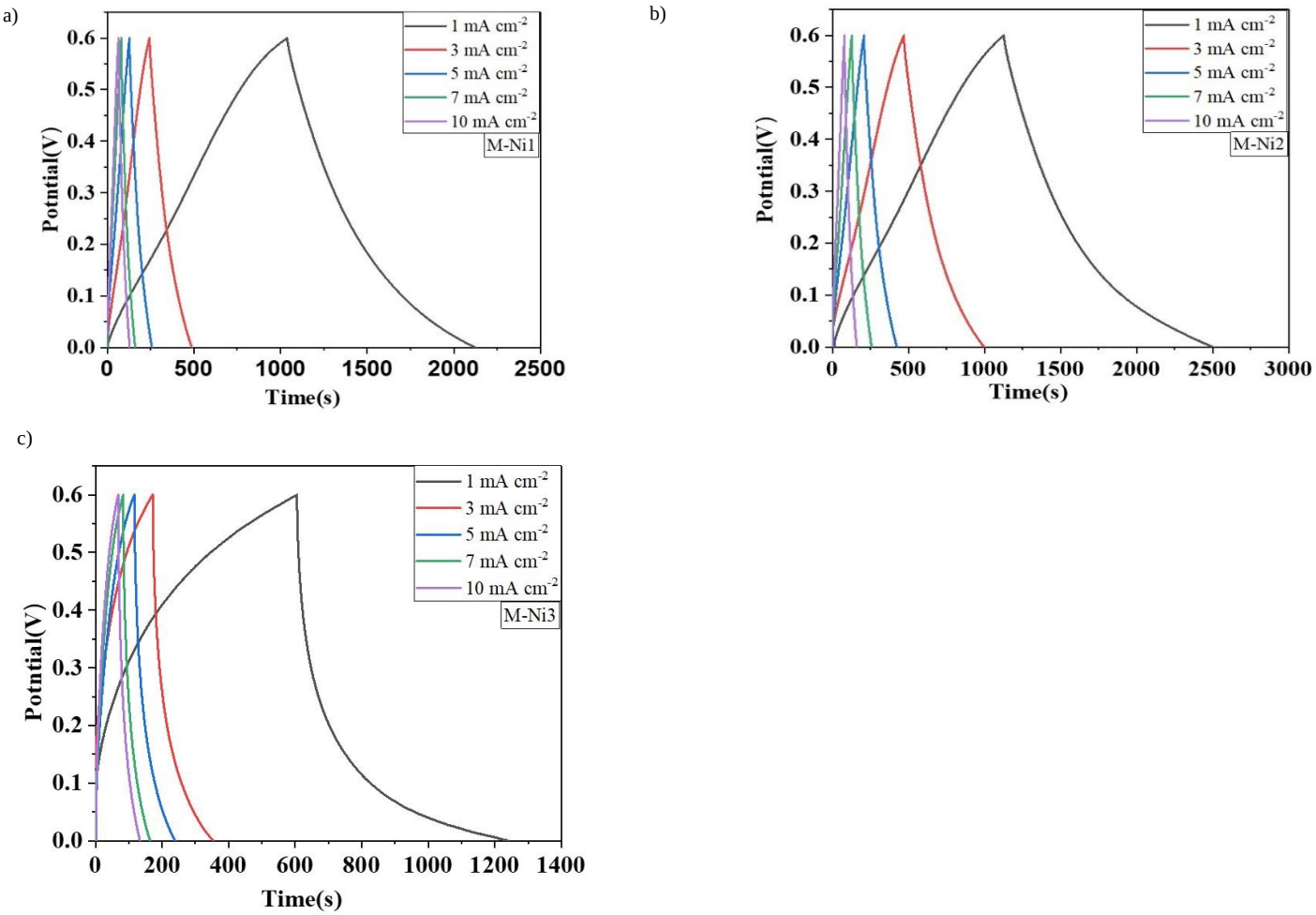

Figure 4. 8: GCD curves at different current density of different electrode concentrations at a) b)M-Ni1,c) M-Ni2, M-Ni3.

Figure 4.9 a) shows the areal capacitance to current density relationship. The areal capacitance is defined as the capacitance per unit area of the electrode and is influenced by the current density, which refers to the current applied per unit area during the charge-discharge process. Typically, at lower current densities, the ions have more time to diffuse into the deeper pores of the electrode material, resulting in higher areal capacitance. As the current density, increases the decrease in penetration time cause less effective use of the active material's lower areal capacitance. At higher current densities, supercapacitors sacrifice energy storage capacity for greater power output, while at lower current densities, they prioritize higher energy storage.

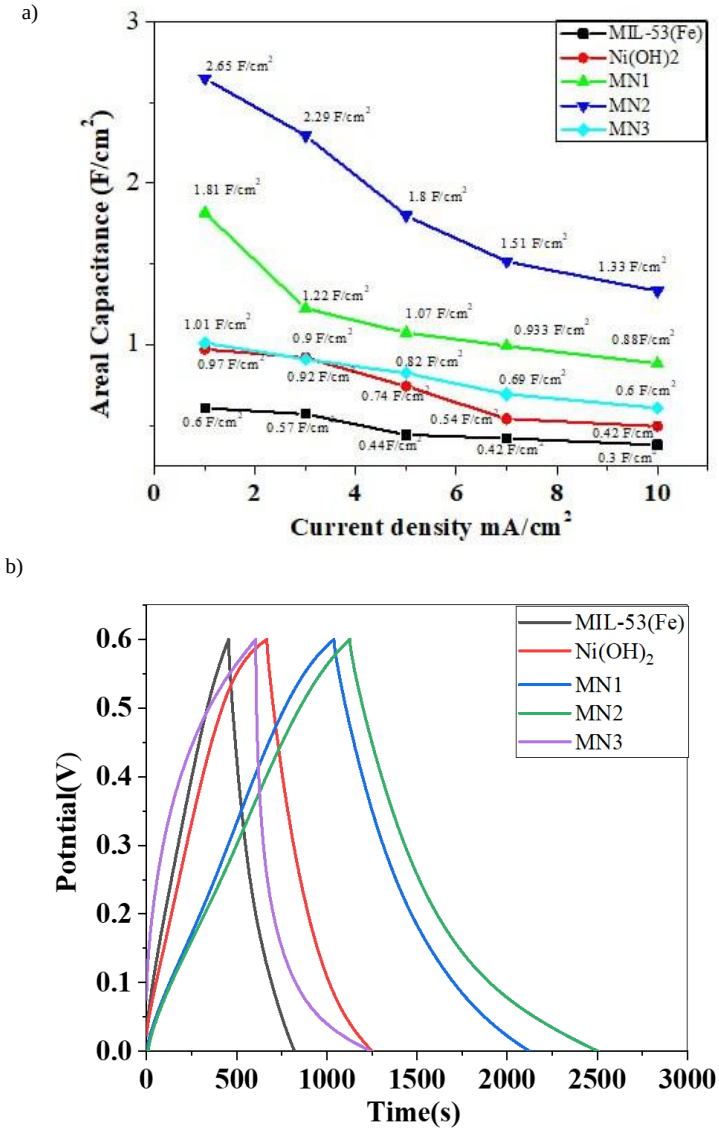

Figure 4. 9: Areal capacitance Vs current density b) GCD curves at 1mA/cm2 for different concentrations of electrode materia

In Figure 4.9 b) Different β-$Ni(OH)_2$ loading on the electrochemical performance of MIL-53(Fe)@ $Ni(OH)_2$ materials, the CV was conducted at a different scan rate between 5mV/s to 200mV/s on M-Ni, M-Ni1, M-Ni2, M-Ni3. The specific capacitance of MIL-53(Fe)/$Ni(OH)_2$ composites is influenced by their surface area, electrical conductivity, and synergy between the two electrode materials. 20% $Ni(OH)_2$ concentration in MIL-53(Fe)/$Ni(OH)_2$ composites delivers the highest specific capacitance. A 20% $Ni(OH)_2$ concentration offers the optimal surface area and porosity for efficient electrolyte access and ion transport. By combining the highest porous structure of MIL-53(Fe) with $Ni(OH)_2$'s excellent redox activity, an increased number of active sites can be achieved. Insufficient $Ni(OH)_2$ can hinder redox reactions due to fewer active sites and a large amount might result in agglomeration or pore blocking, ultimately decreasing the surface area. 20% concentration prevented agglomeration and pore blockage while maintaining a conductive network.

4.5.3. Stability

The long-term cycling performance of the MIL-53(Fe)/$Ni(OH)_2$ was investigated at 15mA/cm^2 for 2000 consecutive cycles. As shown in figure 4.10 the capacitance retention remains 99.2% after 2000 cycles. Furthermore, the inset in figure 4.10 b) shows that the GCD curves of MIL-53(Fe)/$Ni(OH)_2$ after cycling tests change slightly, indicating the remarkable cycling stability.

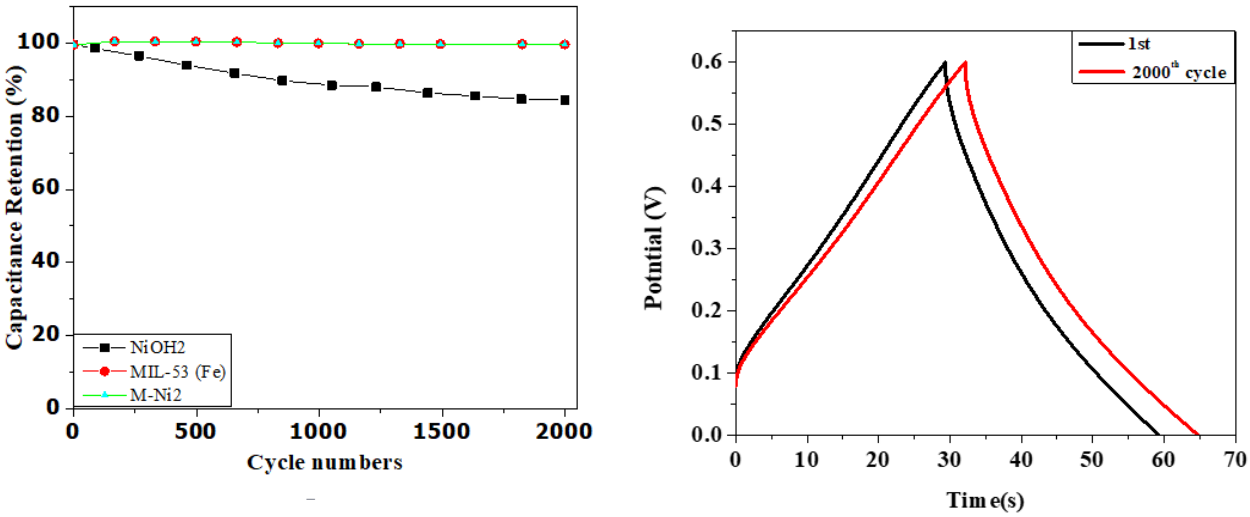

Figure 4. 10: Capacitance retention vs. cycle number of the MIL-53(Fe), β-$Ni(OH)_2$, M-Ni2

The increase in the capacitance retentions of $Ni(OH)_2$ from 84.2% after 2000 cycles in to 99.2% is due to the MOF structure providing mechanical and structural stability by encapsulating the $Ni(OH)_2$ into its structure and also buffers the electrochemical environment, all of which contribute maintain over extended cycling.

4.5.4. Electrochemical impedance spectroscopy

EIS measurement, performed in the frequency range from 100kHz to 10mHz in 1 M Na_2SO_4 in figure 4.10 revealed that the Nyquist plots are similar in shape and comprise a small semicircle at high-frequency region and slope line (Warburg curve) in the low-frequency region. Among them, for the sample M-Ni the Rs related to the internal resistance of electrode material, electrolyte resistance, and contact resistance between the active material and substrate was determined to be 96.17 ohm cm^2, and Rct (charge transfer resistance) value was 83.4 ohm cm^2. The electrochemical impedance spectra of the prepared electrode with different concentration MIL-53(Fe)@ $Ni(OH)_2$ are depicted in Figure 4.9 Rs is the charge-transfer resistance, Cdl is the double-layer capacitance, Wo, is the Warburg element. It can be seen that M-Ni2 has a smaller Rs and Rct. a combination of the contact resistance of the active material with the substance and the test cell to the apparatus, the ionic resistance of the electrolyte, and the intrinsic resistance of the electrode. It is likely that MIL-53(Fe) provide easy transfer access and FeOH ions enhanced the electrical conductivity of $Ni(OH)_2$

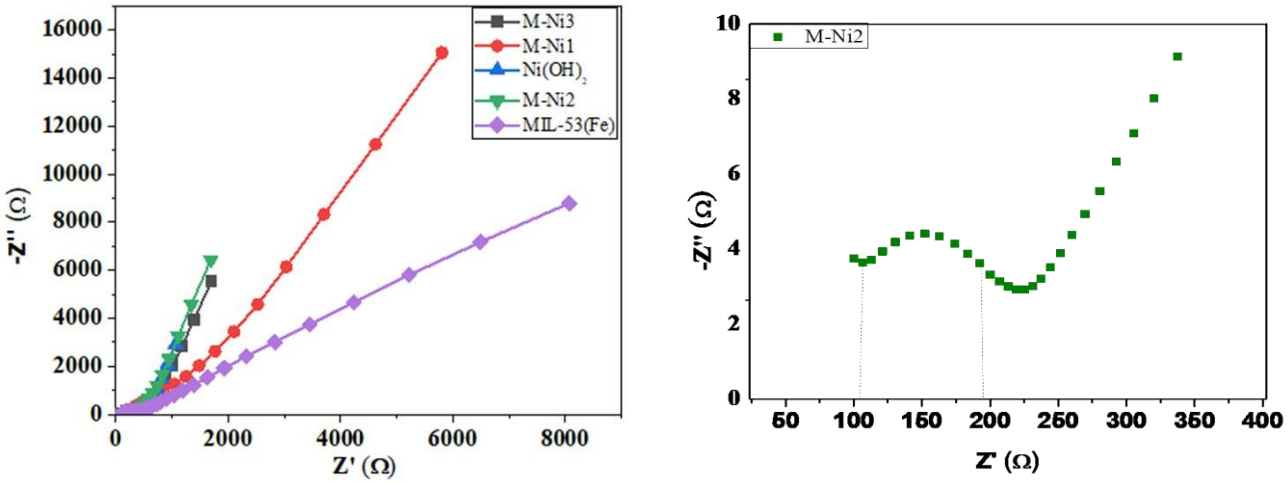

Figure 4. 11: Nyquist plot of MIL-53(Fe), β-Ni(OH)2,M-Ni2

CHAPTER FIVE

5. CONCLUSIONS AND RECOMMENDATIONS

5.1. Conclusions

In this study, MIL-53(Fe)/β-$Ni(OH)_2$ nanocomposites were synthesized through the Sonochemical Wet Impregnation assisted method. The effect of varying the $Ni(OH)_2$ concentration on the electro-performance of the composite has been exploited. Among the concentrations 20% $Ni(OH)_2$ impregnated MIL-53(Fe) exhibits the highest areal capacitance of 2.296 F/cm^2 at 1 mA/cm^2 current density and 99.2% of capacitance retention. This superior performance is attributed to the optimal encapsulation of $Ni(OH)_2$, which enhances the active surface area and leverages the synergistically with other components, improving overall performance through mechanisms like facilitated ion transport effect between β-$Ni(OH)_2$ and the MOF work.

5.2. Recommendations

To enhance the electrochemical performance of MIL-53(Fe)/$Ni(OH)_2$ electrode material in the practical application of supercapacitors, several avenues can be explored. The following recommendations can be implemented to ensure the completion of the research work. Additionally, there are further recommendations for utilizing MIL-53(Fe)/$Ni(OH)_2$ for photocatalyst dye degradations.

- ✓ For which instead of water-based electrolyte system, try to use the organic solvent-based electrolyte system, e.g., Acetonitrile + $TBAPF_6$ in order to check the redox peaks and to increase the energy density of the supercapacitor.
- ✓ In this study, the composite electrode materials have a lower conductivity property so by adding carbon based materials and making it a ternary composite the specific capacitance can be enhanced more than the two composites.
- ✓ Since the electrode material is important, synthesizing a bi-metallic -organic framework can also be beneficial for the performance of supercapacitor.

References

Ali, F., Khalid, N. R., Nabi, G., Ul-Hamid, A., & Ikram, M. (2021). Hydrothermal synthesis of cerium-doped Co3O4 nanoflakes as electrode for supercapacitor application. *International Journal of Energy Research*, *45*(2), 1999-2010.

Arbizzani, C., Mastragostino, M., & Soavi, F. (2001). New trends in electrochemical supercapacitors. *Journal of power sources*, *100*(1), 164-170. https://doi.org/https://doi.org/10.1016/S0378-7753(01)00892-8

Areir, M., Xu, Y., Harrison, D., & Fyson, J. (2017). 3D printing of highly flexible supercapacitor designed for wearable energy storage. *Materials Science and Engineering: B*, *226*, 29-38. https://doi.org/https://doi.org/10.1016/j.mseb.2017.09.004

Armand, M., & Tarascon, J.-M. (2008). Building better batteries. *Nature*, *451*(7179), 652-657.

Arulepp, M., Leis, J., Lätt, M., Miller, F., Rumma, K., Lust, E., & Burke, A. F. (2006). The advanced carbide-derived carbon based supercapacitor. *Journal of power sources*, *162*(2), 1460-1466. https://doi.org/https://doi.org/10.1016/j.jpowsour.2006.08.014

Asghar, G., Fiaz, M., Farid, M. A., Ashiq, M. N., & Athar, M. (2024). Synthesis of the highly efficient catalysts CdZnS@MIL-53(Fe) and ZnS@MIL-53(Fe) and their thermally decomposed derivative for electrochemical OER activity and photodegradation of Rhodamine B dye. *International Journal of Hydrogen Energy*, *51*, 1435-1447. https://doi.org/10.1016/j.ijhydene.2023.09.208

Augustyn, V., Simon, P., & Dunn, B. (2014). Pseudocapacitive oxide materials for high-rate electrochemical energy storage. *Energy & Environmental Science*, *7*, 1597. https://doi.org/10.1039/c3ee44164d

Bae, J.-S., Hong, S. Y., Park, J. C., Rhim, G. B., Youn, M. H., Jeong, H., Kang, S. W., Yang, J.-I., Jung, H., & Chun, D. H. (2019). Eco-friendly prepared iron-ore-based catalysts for Fischer-Tropsch synthesis. *Applied Catalysis B: Environmental*, *244*, 576-582. https://doi.org/https://doi.org/10.1016/j.apcatb.2018.11.082

Bahadori, M., & Dehghani-sanij, A. (2014). *Wind Towers Architecture, Climate and Sustainability*. https://doi.org/10.1007/978-3-319-05876-4

Barbieri, O., Hahn, M., Herzog, A., & Kötz, R. (2005). Capacitance limits of high surface area activated carbons for double layer capacitors. *Carbon, 43*, 1303-1310. https://doi.org/10.1016/j.carbon.2005.01.001

Bernard, M. C., Cortes, R., Keddam, M., Takenouti, H., Bernard, P., & Senyarich, S. (1996). Structural defects and electrochemical reactivity of β-Ni(OH)2. *Journal of power sources*, *63*(2), 247-254. https://doi.org/https://doi.org/10.1016/S0378-7753(96)02482-2

Boicea, V. A. (2014). Energy Storage Technologies: The Past and the Present. *Proceedings of the IEEE*, *102*(11), 1777-1794. https://doi.org/10.1109/jproc.2014.2359545

Burke, A. (2007). R&D considerations for the performance and application of electrochemical capacitors. *Electrochimica Acta*, *53*(3), 1083-1091. https://doi.org/https://doi.org/10.1016/j.electacta.2007.01.011

Burke, A., & Zhao, H. (2015). *Present and Future Applications of Supercapacitors in Electric and Hybrid Vehicles*. https://doi.org/10.1109/VTCFall.2015.7391093

Burke, A. F. (2011). Materials Research for High Energy Density Electrochemical Capacitor. *MRS Online Proceedings Library*, *1100*(1), 7. https://doi.org/10.1557/PROC-1100-JJ06-02

Cao, Z., Momen, R., Tao, S., Xiong, D., Song, Z., Xiao, X., Deng, W., Hou, H., Yasar, S., Altin, S., Bulut, F., Zou, G., & Ji, X. (2022). Metal-Organic Framework Materials for Electrochemical Supercapacitors. *Nanomicro Lett*, *14*(1), 181. https://doi.org/10.1007/s40820-022-00910-9

Carignano, M. G., Costa-Castelló, R., Roda, V., Nigro, N. M., Junco, S., & Feroldi, D. (2017). Energy management strategy for fuel cell-supercapacitor hybrid vehicles based on prediction of energy demand. *Journal of power sources*, *360*, 419-433.

Chameh, B., Moradi Alborzi, M., Hajati, S., Hessari, F. A., & Kiani, M. A. (2021). Synthesis and Characterization of Palladium Impregnated MIL-53(Fe) as Cathode Material of Supercapacitor. *Advanced Ceramics Progress*, *7*(1), 11-17. https://doi.org/10.30501/acp.2020.250166.1045

Chen, C., Zhang, M., Guan, Q., & Li, W. (2012). Kinetic and thermodynamic studies on the adsorption of xylenol orange onto MIL-101 (Cr). *Chemical Engineering Journal*, *183*, 60-67.

Chen, W., Fan, Z., Gu, L., Bao, X., & Wang, C. (2010). Enhanced capacitance of manganese oxide via confinement inside carbon nanotubes. *Chemical communications (Cambridge, England)*, *46*, 3905-3907. https://doi.org/10.1039/c000517g

Chen, W., Fan, Z., Gu, L., Bao, X., & Wang, C. (2010). Enhanced capacitance of manganese oxide via confinement inside carbon nanotubes [10.1039/C000517G]. *Chemical Communications*, *46*(22), 3905-3907. https://doi.org/10.1039/C000517G

Chen, Y., Kang, C., Ma, L., Fu, L., Li, G., Hu, Q., & Liu, Q. (2021). MOF-derived Fe2O3 decorated with MnO2 nanosheet arrays as anode for high energy density hybrid supercapacitor. *Chemical Engineering Journal*, *417*, 129243. https://doi.org/https://doi.org/10.1016/j.cej.2021.129243

Chen, Z., Chen, J., & Li, Y. (2017). Metal–organic-framework-based catalysts for hydrogenation reactions. *Chinese Journal of Catalysis*, *38*(7), 1108-1126. https://doi.org/https://doi.org/10.1016/S1872-2067(17)62852-3

Chmiola, J., Yushin, G., Dash, R., & Gogotsi, Y. (2006). Effect of pore size and surface area of carbide derived carbons on specific capacitance. *Journal of power sources*, *158*(1), 765-772. https://doi.org/https://doi.org/10.1016/j.jpowsour.2005.09.008

Chmiola, J., Yushin, G., Dash, R., Hoffman, E., Fischer, J., Barsoum, M., & Gogotsi, Y. (2005). Double-Layer Capacitance of Carbide Derived Carbons in Sulfuric Acid. *Electrochemical and Solid-State Letters*, *8*. https://doi.org/10.1149/1.1921134

Chmiola, J., Yushin, G., Gogotsi, Y., Portet, C., Simon, P., & Taberna, P. L. (2006). Anomalous Increase in Carbon Capacitance at Pore Sizes Less Than 1 Nanometer. *Science*, *313*(5794), 1760-1763. https://doi.org/doi:10.1126/science.1132195

Choi, J. W., & Aurbach, D. (2016). Promise and reality of post-lithium-ion batteries with high energy densities. *Nature Reviews Materials*, *1*(4), 16013. https://doi.org/10.1038/natrevmats.2016.13

Chu, J., Li, X., Li, Q., Ma, J., Wu, B., Wang, X., Zhang, R., Gong, M., & Xiong, S. (2020). Hydrothermal synthesis of PANI nanowires for high-performance supercapacitor. *High Performance Polymers*, *32*(3), 258-267.

Cosimbescu, L., Merkel, D. R., Darsell, J., & Petrossian, G. (2021). Simple But Tricky: Investigations of Terephthalic Acid Purity Obtained from Mixed PET Waste.

Industrial & Engineering Chemistry Research, *60*(35), 12792-12797. https://doi.org/10.1021/acs.iecr.1c02604

Czagany, M., Hompoth, S., Keshri, A. K., Pandit, N., Galambos, I., Gacsi, Z., & Baumli, P. (2024). Supercapacitors: An Efficient Way for Energy Storage Application. *Materials*, *17*(3), 702. https://www.mdpi.com/1996-1944/17/3/702

Dai, L., Chang, D. W., Baek, J. B., & Lu, W. (2012). Carbon nanomaterials for advanced energy conversion and storage. *small*, *8*(8), 1130-1166.

Dargahi, R., Ebrahimzadeh, H., Asgharinezhad, A. A., Hashemzadeh, A., & Amini, M. M. (2018). Dispersive magnetic solid-phase extraction of phthalate esters from water samples and human plasma based on a nanosorbent composed of MIL-101 (Cr) metal–organic framework and magnetite nanoparticles before their determination by GC–MS. *Journal of separation science*, *41*(4), 948-957.

Deep, A., Bhardwaj, S. K., Paul, A. K., Kim, K. H., & Kumar, P. (2015). Surface assembly of nano-metal organic framework on amine functionalized indium tin oxide substrate for impedimetric sensing of parathion. *Biosens Bioelectron*, *65*, 226-231. https://doi.org/10.1016/j.bios.2014.10.045

Dehghani-Sanij, A. R., Dehghani, S. R., Naterer, G. F., & Muzychka, Y. S. (2017). Marine icing phenomena on vessels and offshore structures: Prediction and analysis. *Ocean Engineering*, *143*, 1-23. https://doi.org/https://doi.org/10.1016/j.oceaneng.2017.07.049

Dehghani-sanij, A. R., Soltani, M., & Raahemifar, K. (2015). A new design of wind tower for passive ventilation in buildings to reduce energy consumption in windy regions. *Renewable and Sustainable Energy Reviews*, *42*, 182-195. https://doi.org/https://doi.org/10.1016/j.rser.2014.10.018

Deka, B. K., Hazarika, A., Kim, J., Park, Y.-B., & Park, H. W. (2017). Recent development and challenges of multifunctional structural supercapacitors for automotive industries. *International Journal of Energy Research*, *41*(10), 1397-1411. https://doi.org/https://doi.org/10.1002/er.3707

Dey, C., Kundu, T., & Banerjee, R. (2012). Reversible phase transformation in proton conducting Strandberg-type POM based metal organic material [10.1039/C1CC15162B]. *Chemical Communications*, *48*(2), 266-268. https://doi.org/10.1039/C1CC15162B

Du, L., Lin, H., Ma, Z., Wang, Q., Li, D., Shen, Y., Zhang, W., Rui, K., Zhu, J., & Huang, W. (2019). Using and recycling V2O5 as high performance anode materials for sustainable lithium ion battery. *Journal of power sources*, *424*, 158-164. https://doi.org/https://doi.org/10.1016/j.jpowsour.2019.03.103

Du, M., Li, Q., Zhao, Y., Liu, C.-S., & Pang, H. (2020). A review of electrochemical energy storage behaviors based on pristine metal–organic frameworks and their composites. *Coordination Chemistry Reviews*, *416*. https://doi.org/10.1016/j.ccr.2020.213341

Dubal, D. P., Kim, J. G., Kim, Y., Holze, R., & Kim, W. B. (2013). Demonstrating the Highest Supercapacitive Performance of Branched MnO2 Nanorods Grown Directly on Flexible Substrates using Controlled Chemistry at Ambient Temperature. *Energy Technology*, *1*(2-3), 125-130. https://doi.org/https://doi.org/10.1002/ente.201200040

El-Shahat, M., Mochtar, M., Rashad, M. M., & Mousa, M. A. (2020). Single and ternary nanocomposite electrodes of Mn3O4/TiO2/rGO for supercapacitors. *Journal of Solid State Electrochemistry*, *25*(3), 803-819. https://doi.org/10.1007/s10008-020-04837-2

Férey, G. (2008). Hybrid porous solids: past, present, future. *Chemical Society Reviews*, *37*(1), 191-214.

Flores, J. G., Delgado-García, R., & Sánchez-Sánchez, M. (2022). Semiamorphous Fe-BDC: The missing link between the highly-demanded iron carboxylate MOF catalysts. *Catalysis Today*, *390-391*, 237-245. https://doi.org/https://doi.org/10.1016/j.cattod.2021.11.004

Frackowiak, E., & Beguin, F. (2001). Carbon Materials for the Electrochemical Storage of Energy in Capacitors. *Carbon*, *39*, 937-950. https://doi.org/10.1016/S0008-6223(00)00183-4

Furukawa, H., & Yaghi, O. M. (2009). Storage of hydrogen, methane, and carbon dioxide in highly porous covalent organic frameworks for clean energy applications. *J Am Chem Soc*, *131*(25), 8875-8883. https://doi.org/10.1021/ja9015765

Galiński, M., Lewandowski, A., & Stępniak, I. (2006). Ionic liquids as electrolytes. *Electrochimica Acta*, *51*(26), 5567-5580.

Gamil, S., El Rouby, W., Antuch, M., & Zedan, I. (2019). Nanohybrid layered double hydroxide materials as efficient catalysts for methanol electrooxidation. *RSC Advances*, *9*, 13503-13514. https://doi.org/10.1039/C9RA01270B

Gogotsi, Y., & Penner, R. M. (2018). Energy Storage in Nanomaterials – Capacitive, Pseudocapacitive, or Battery-like? *ACS Nano*, *12*(3), 2081-2083. https://doi.org/10.1021/acsnano.8b01914

Granato, T., Testa, F., & Olivo, R. (2012). Catalytic activity of HKUST-1 coated on ceramic foam. *Microporous and mesoporous materials*, *153*, 236-246.

Gui, Q., Ba, D., Li, L., Liu, W., Li, Y., & Liu, J. (2022). Recent advances in materials and device technologies for aqueous hybrid supercapacitors. *Science China Materials*, *65*(1), 10-31. https://doi.org/10.1007/s40843-021-1733-1

Guney, M. S., & Tepe, Y. (2017). Classification and assessment of energy storage systems. *Renewable and Sustainable Energy Reviews*, *75*, 1187-1197. https://doi.org/https://doi.org/10.1016/j.rser.2016.11.102

Gurav, K. V., Patil, U. M., Shin, S. W., Agawane, G. L., Suryawanshi, M. P., Pawar, S. M., Patil, P. S., Lokhande, C. D., & Kim, J. H. (2013). Room temperature chemical synthesis of Cu(OH)2 thin films for supercapacitor application. *Journal of Alloys and Compounds*, *573*, 27-31. https://doi.org/https://doi.org/10.1016/j.jallcom.2013.03.193

Haile, S. M. (2003). Fuel cell materials and components. *Acta materialia*, *51*(19), 5981-6000.

Haque, E., & Jhung, S. H. (2011). Synthesis of isostructural metal–organic frameworks, CPO-27s, with ultrasound, microwave, and conventional heating: Effect of synthesis methods and metal ions. *Chemical Engineering Journal*, *173*(3), 866-872. https://doi.org/https://doi.org/10.1016/j.cej.2011.08.037

Hartmann, B., Prikler, L., & Varjasi, I. (2017, 18-22 June 2017). Revealing technological possibilities of recovering braking energy of electric traction vehicles. 2017 IEEE Manchester PowerTech,

Herrero, E., Buller, L. J., & Abruña, H. D. (2001). Underpotential deposition at single crystal surfaces of Au, Pt, Ag and other materials. *Chem Rev*, *101*(7), 1897-1930. https://doi.org/10.1021/cr9600363

Hirchenhofer, J., Stauffer, D., Englman, R., & Klett, M. (1998). Fuel cell handbook.

Hirscher, M., & Panella, B. (2007). Hydrogen storage in metal–organic frameworks. *Scripta Materialia*, *56*(10), 809-812. https://doi.org/https://doi.org/10.1016/j.scriptamat.2007.01.005

Holze, R. (2015). F. Béguin, E. Frąckowiak (eds): Supercapacitors – Materials, Systems, and Applications. *Journal of Solid State Electrochemistry*, *19*. https://doi.org/10.1007/s10008-014-2718-2

Hu, C.-C., & Tsou, T.-W. (2002). Ideal capacitive behavior of hydrous manganese oxide prepared by anodic deposition. *Electrochemistry Communications*, *4*(2), 105-109. https://doi.org/https://doi.org/10.1016/S1388-2481(01)00285-5

Hussain, M., Alotaibi, B., Alrowaily, A. W., Alyousef, H. A., Alotiby, M. F., Abdullah, M., Al-Sehemi, A. G., Henaish, A., Ahmad, Z., & Aman, S. (2024). Synthesis of high-performance supercapacitor electrode materials by hydrothermal route based on ZnSe/MnSe composite. *Journal of Physics and Chemistry of Solids*, *188*, 111919.

Inagaki, M., Konno, H., & Tanaike, O. (2010). Carbon materials for electrochemical capacitors. *Journal of power sources*, *195*(24), 7880-7903. https://doi.org/https://doi.org/10.1016/j.jpowsour.2010.06.036

Iqbal, J., Bashir, S., Ansari, M. O., Jafer, R., Jilani, A., Mohammad, S., Ramesh, K., & Ramesh, S. (2021). Chapter seven - Ternary nanocomposites for supercapattery. In N. Arshid, M. Khalid, & A. N. Grace (Eds.), *Advances in Supercapacitor and Supercapattery* (pp. 141-173). Elsevier. https://doi.org/https://doi.org/10.1016/B978-0-12-819897-1.00013-6

Iqbal, M. Z., Zakar, S., & Haider, S. S. (2020). Role of aqueous electrolytes on the performance of electrochemical energy storage device. *Journal of Electroanalytical Chemistry*, *858*, 113793. https://doi.org/https://doi.org/10.1016/j.jelechem.2019.113793

Ishikawa, M., Sakamoto, A., Monta, M., Matsuda, Y., & Ishida, K. (1996). Effect of treatment of activated carbon fiber cloth electrodes with cold plasma upon performance of electric double-layer capacitors. *Journal of power sources*, *60*(2), 233-238. https://doi.org/https://doi.org/10.1016/S0378-7753(96)80016-4

Jänes, A., Permann, L., Arulepp, M., & Lust, E. (2004). Electrochemical characteristics of nanoporous carbide-derived carbon materials in non-aqueous electrolyte solutions. *Electrochemistry Communications*, *6*(3), 313-318. https://doi.org/https://doi.org/10.1016/j.elecom.2004.01.009

Jänes, A., Permann, L., Arulepp, M., & Lust, E. (2004). Electrochemical characteristics of nanoporous carbide-derived carbon materials in non-aqueous electrolyte solutions. *Electrochemistry Communications - ELECTROCHEM COMMUN*, *6*, 313-318. https://doi.org/10.1016/j.elecom.2004.01.009

Jarvis, K., Deng, Z., Allard, L., Manthiram, A., & Ferreira, P. (2011). Atomic Structure of a Lithium-Rich Layered Oxide Material for Lithium-Ion Batteries: Evidence of a Solid Solution. *Chem. Mater., 23(16)*. https://doi.org/10.1021/cm200831c

Kale, M. B., Borse, R. A., Gomaa Abdelkader Mohamed, A., & Wang, Y. (2021). Electrocatalysts by electrodeposition: recent advances, synthesis methods, and applications in energy conversion. *Advanced Functional Materials*, *31*(25), 2101313.

Karthikeyan, S., Narenthiran, B., Sivanantham, A., Bhatlu, L. D., & Maridurai, T. (2021). Supercapacitor: Evolution and review. *Materials Today: Proceedings*, *46*, 3984-3988. https://doi.org/10.1016/j.matpr.2021.02.526

Kerns, J. (2015). What's the Difference between Batteries and Capacitors. *Machine Design*.

Kim, H., Hong, J., Park, K.-Y., Kim, H., Kim, S.-W., & Kang, K. (2014). Aqueous rechargeable Li and Na ion batteries. *Chemical Reviews*, *114*(23), 11788-11827.

Kim, J., Yang, S.-T., Choi, S. B., Sim, J., Kim, J., & Ahn, W.-S. (2011). Control of catenation in CuTATB-n metal–organic frameworks by sonochemical synthesis and its effect on CO2 adsorption [10.1039/C0JM03318A]. *Journal of Materials Chemistry*, *21*(9), 3070-3076. https://doi.org/10.1039/C0JM03318A

Kim, Y. J., Horie, Y., Ozaki, S., Matsuzawa, Y., Suezaki, H., Kim, C., Miyashita, N., & Endo, M. (2004). Correlation between the pore and solvated ion size on capacitance uptake of PVDC-based carbons. *Carbon*, *42*(8), 1491-1500. https://doi.org/https://doi.org/10.1016/j.carbon.2004.01.049

Kitagawa, S., Kitaura, R., & Noro, S. i. (2004). Functional porous coordination polymers. *Angewandte Chemie International Edition*, *43*(18), 2334-2375.

Kötz, R., & Carlen, M. (2000). Principles and applications of electrochemical capacitors. *Electrochimica Acta*, *45*(15), 2483-2498. https://doi.org/https://doi.org/10.1016/S0013-4686(00)00354-6

Krause, A., Kossyrev, P., Oljaca, M., Passerini, S., Winter, M., & Balducci, A. (2011). Electrochemical double layer capacitor and lithium-ion capacitor based on carbon

black. *Journal of power sources*, *196*(20), 8836-8842. https://doi.org/https://doi.org/10.1016/j.jpowsour.2011.06.019

Kumar, P., Deep, A., & Kim, K.-H. (2015). Metal organic frameworks for sensing applications. *TrAC Trends in Analytical Chemistry*, *73*, 39-53. https://doi.org/https://doi.org/10.1016/j.trac.2015.04.009

Kurzweil, P., & Chwistek, M. (2008). Electrochemical stability of organic electrolytes in supercapacitors: Spectroscopy and gas analysis of decomposition products. *Journal of power sources*, *176*(2), 555-567. https://doi.org/https://doi.org/10.1016/j.jpowsour.2007.08.070

Lee, J. H., Ahn, Y., & Kwak, S. Y. (2022). Facile Sonochemical Synthesis of Flexible Fe-Based Metal-Organic Frameworks and Their Efficient Removal of Organic Contaminants from Aqueous Solutions. *ACS Omega*, *7*(27), 23213-23222. https://doi.org/10.1021/acsomega.2c01068

Lee, Y.-R., Jang, M.-S., Cho, H.-Y., Kwon, H.-J., Kim, S., & Ahn, W.-S. (2015). ZIF-8: A comparison of synthesis methods. *Chemical Engineering Journal*, *271*, 276-280. https://doi.org/https://doi.org/10.1016/j.cej.2015.02.094

Li, H., Eddaoudi, M., O'Keeffe, M., & Yaghi, O. M. (1999). Design and synthesis of an exceptionally stable and highly porous metal-organic framework. *nature*, *402*(6759), 276-279.

Li, H., Li, L., Lin, R.-B., Zhou, W., Zhang, Z., Xiang, S., & Chen, B. (2019). Porous metal-organic frameworks for gas storage and separation: Status and challenges. *EnergyChem*, *1*(1), 100006.

Li, J., Zhong, L., Li, J.-x., Wu, H.-f., Shao, W.-w., Wang, P.-q., Liu, M.-q., Zhang, G., & Jing, M.-x. (2023). Insights into the effects of different inorganic fillers on the electrochemical performances of polymer solid electrolytes. *Colloids and Surfaces A: Physicochemical and Engineering Aspects*, *671*, 131704. https://doi.org/https://doi.org/10.1016/j.colsurfa.2023.131704

Li, M., Zhou, M., Wen, Z. Q., & Zhang, Y. X. (2017). Flower-like NiFe layered double hydroxides coated MnO2 for high-performance flexible supercapacitors. *Journal of Energy Storage*, *11*, 242-248. https://doi.org/https://doi.org/10.1016/j.est.2017.03.010

Li, S.-H., Liu, Q.-H., Qi, L., Lu, L.-H., & Wang, H.-Y. (2012). Progress in Research on Manganese Dioxide Electrode Materials for Electrochemical Capacitors. *Chinese Journal of Analytical Chemistry*, *40*(3), 339-346. https://doi.org/https://doi.org/10.1016/S1872-2040(11)60534-3

Liu, J., Lu, S., Wang, L., Xie, F., Shang, W., & Wen, Y. (2023). Constructed a bimetallic synergistic organic backbones electrode by the electrochemical deposition for high-performance flexible supercapacitors. *Journal of Energy Storage*, *68*, 107885.

Liu, J., Xia, H., Xue, D., & Lu, L. (2009). Double-shelled nanocapsules of V2O5-based composites as high-performance anode and cathode materials for Li ion batteries. *J Am Chem Soc*, *131*(34), 12086-12087. https://doi.org/10.1021/ja9053256

Liu, S., Huo, Q., Chen, R., Chen, P., Li, Y., & Han, Y. (2015). Synthesis and Characterization of an Iron Nitride Constructed by a Novel Template of Metal Organic Framework. *Journal of Spectroscopy*, *2015*, 1-8. https://doi.org/10.1155/2015/362103

Liu, Y., Wang, B., Ma, S., Yu, T., Xu, X., Li, Q., Wang, S., Han, Y., Yu, Z., & Zhu, J. (2021). Catalyst-free malleable, degradable, bio-based epoxy thermosets and its application in recyclable carbon fiber composites. *Composites Part B: Engineering*, *211*, 108654. https://doi.org/https://doi.org/10.1016/j.compositesb.2021.108654

Llewellyn, P. L., Bourrelly, S., Serre, C., Vimont, A., Daturi, M., Hamon, L., De Weireld, G., Chang, J.-S., Hong, D.-Y., & Kyu Hwang, Y. (2008). High uptakes of CO2 and CH4 in mesoporous metal□ organic frameworks mil-100 and mil-101. *Langmuir*, *24*(14), 7245-7250.

Lu, P., Xue, D., Yang, H., & Liu, Y. (2013). Supercapacitor and nanoscale research towards electrochemical energy storage. *International Journal of Smart and Nano Materials*, *4*(1), 2-26. https://doi.org/10.1080/19475411.2011.652218

Lu, X., Yu, M., Tong, Y., & Li, Y. (2014). Flexible solid-state supercapacitors: Design, fabrication and applications. *Energy & Environmental Science*, *7*, 2160. https://doi.org/10.1039/c4ee00960f

Lu, Y., Dong, Y., Jiang, H., Wang, Z., Cao, Z., Guo, S., Wang, T., Li, T., & Liaw, P. K. (2020). Promising properties and future trend of eutectic high entropy alloys. *Scripta Materialia*, *187*, 202-209. https://doi.org/https://doi.org/10.1016/j.scriptamat.2020.06.022

Lu, Y., Zhao, Y., Zhao, X., Li, G., & Zhang, C. (2017). Status analysis of regenerative braking energy utilization equipments in urban rail transit. 2017 IEEE transportation electrification conference and expo, Asia-Pacific (ITEC Asia-Pacific),

Ma, L., Chen, R., Hu, Y., Zhang, W., Zhu, G., Zhao, P., Chen, T., Wang, C., Yan, W., Wang, Y., Wang, L., Tie, Z., Liu, J., & Jin, Z. (2018). Nanoporous and lyophilic battery separator from regenerated eggshell membrane with effective suppression of dendritic lithium growth. *Energy Storage Materials*, *14*, 258-266. https://doi.org/https://doi.org/10.1016/j.ensm.2018.04.016

Mahmoodi, N. M., Abdi, J., Oveisi, M., Asli, M. A., & Vossoughi, M. (2018). Metal-organic framework (MIL-100 (Fe)): Synthesis, detailed photocatalytic dye degradation ability in colored textile wastewater and recycling. *Materials Research Bulletin*, *100*, 357-366.

Mekhilef, S., Saidur, R., & Safari, A. (2012). Comparative study of different fuel cell technologies. *Renewable and Sustainable Energy Reviews*, *16*(1), 981-989.

Millange, F., Guillou, N., Walton, R. I., Grenèche, J.-M., Margiolaki, I., & Férey, G. (2008). Effect of the nature of the metal on the breathing steps in MOFs with dynamic frameworks [10.1039/B809419E]. *Chemical Communications*(39), 4732-4734. https://doi.org/10.1039/B809419E

Mohamed, M. R., Leung, P. K., & Sulaiman, M. H. (2015). Performance characterization of a vanadium redox flow battery at different operating parameters under a standardized test-bed system. *Applied Energy*, *137*. https://doi.org/10.1016/j.apenergy.2014.10.042

Mohammed, L., Mengyang, H., Hamenu, L., Madzvamuse, A., Nyamful, A., Dodoo Arhin, D., Danquah, A., Odoi, K., Zainudeen, N., Darkwa, S., & Park, J. h. (2021). Preparation of Vapor Grown Carbon Fiber/2-((4- dimethylamino) phenyl) amino) naphthalene-1, 4-dione Composites and their supercapacitor properties. *International Journal of Electrochemical Science*, *16*, 210756. https://doi.org/10.20964/2021.07.51

Mohanraj, M., Shaji, S. P., Rajni, K. S., & Ulaganathan, M. (2024). β-Ni(OH)2 / WC for high-energy aqueous hybrid supercapacitor. *Electrochimica Acta*, *482*, 143972. https://doi.org/https://doi.org/10.1016/j.electacta.2024.143972

Mostaanzadeh, H., Shahmohammadi, M., Ehsani, A., Moharramnejad, M., & Honarmand, E. (2021). Green-synthesized Zn-BTC metal–organic frameworks as a highly efficient

material to improving electrochemical pseudocapacitance performance of P-type conductive polymer. *Journal of Materials Science: Materials in Electronics*, *32*(22), 26539-26547. https://doi.org/10.1007/s10854-021-07030-x

Muhammad Ikram, Y. J., Naveed Akhtar Shad, Muhammad Munir Sajid, Muhammad Irfan, Anam Munawar, Tousif Hussain, Muhammad Imran, Dilshad Hussain. (2021). Facile hydrothermal synthesis of nickel tungstate (NiWO4) nanostructures with pronounced supercapacitor and electrochemical sensing activities. *Journal of Alloys and Compounds*, *Volume 878*, Article 160314. https://doi.org/10.1016/j.jallcom.2021.160314

Nagarajarao, S. H., Nandagudi, A., Viswanatha, R., Basavaraja, B. M., Santosh, M. S., Praveen, B. M., & Pandith, A. (2022). Recent Developments in Supercapacitor Electrodes: A Mini Review. *ChemEngineering*, *6*(1). https://doi.org/10.3390/chemengineering6010005

Naoi, K., & Simon, P. (2008). New Materials and New Configurations for Advanced Electrochemical Capacitors. *The Electrochemical Society Interface*, *17*(1), 34. https://doi.org/10.1149/2.F04081IF

Naser, S. A. E., Badmus, K. O., & Khotseng, L. (2023). Synthesis, Properties, and Applications of Metal Organic Frameworks Supported on Graphene Oxide. *Coatings*, *13*(8), 1456. https://www.mdpi.com/2079-6412/13/8/1456

Nidhi Tiwari, S. K., Rahul Ingole, Shrinivas Kulkarni. (2022). Facile hydrothermal synthesis of ZnFe2O4 nanostructures for high-performance supercapacitor application. *Ceramics International*, *48*(19), 29478-29483. https://doi.org/10.1016/j.ceramint.2022.06.276

Nithya, V. D., Kalai Selvan, R., Kalpana, D., Vasylechko, L., & Sanjeeviraja, C. (2013). Synthesis of Bi2WO6 nanoparticles and its electrochemical properties in different electrolytes for pseudocapacitor electrodes. *Electrochimica Acta*, *109*, 720-731. https://doi.org/https://doi.org/10.1016/j.electacta.2013.07.138

Nivetha, R., Kollu, P., Nagamuthu Raja, K. C., Sudhagar, P., Jeong, S., & Grace, A. (2019). Role of MIL-53(Fe)/hydrated–dehydrated MOF catalyst for electrochemical hydrogen evolution reaction (HER) in alkaline medium and photocatalysis. *RSC Advances*, *9*, 3215-3223. https://doi.org/10.1039/C8RA08208A

Omanda, H., Brousse, T., Marhic, C., & Schleich, D. (2004). Improvement of the Thermal Stability of LiNi0. 8Co0. 2 O 2 Cathode by a SiO x Protective Coating. *Journal of the Electrochemical Society*, *151*(6), A922.

Pal, B., Yang, S., Ramesh, S., Thangadurai, V., & Jose, R. (2019). Electrolyte selection for supercapacitive devices: A critical review. *Nanoscale Advances*, *1*. https://doi.org/10.1039/C9NA00374F

Pal, B., Yang, S., Ramesh, S., Thangadurai, V., & Jose, R. (2019). Electrolyte selection for supercapacitive devices: a critical review. *Nanoscale Adv*, *1*(10), 3807-3835. https://doi.org/10.1039/c9na00374f

Pan, Z., Yu, S., Wang, L., Li, C., Meng, F., Wang, N., Zhou, S., Xiong, Y., Wang, Z., Wu, Y., Liu, X., Fang, B., & Zhang, Y. (2023). Recent Advances in Porous Carbon Materials as Electrodes for Supercapacitors. *Nanomaterials (Basel)*, *13*(11). https://doi.org/10.3390/nano13111744

Panda, P. K., Grigoriev, A., Mishra, Y. K., & Ahuja, R. (2020). Progress in supercapacitors: roles of two dimensional nanotubular materials. *Nanoscale Advances*, *2*(1), 70-108.

Pandolfo, A. G., & Hollenkamp, A. F. (2006). Carbon properties and their role in supercapacitors. *Journal of power sources*, *157*(1), 11-27. https://doi.org/https://doi.org/10.1016/j.jpowsour.2006.02.065

Patra, A., K, N., Jose, J. R., Sahoo, S., Chakraborty, B., & Rout, C. S. (2021). Understanding the charge storage mechanism of supercapacitors:in situ/operandospectroscopic approaches and theoretical investigations. *Journal of materials chemistry A*, *9*(46), 25852-25891. https://doi.org/10.1039/d1ta07401f

Pérez-Lombard, L., Ortiz, J., & Pout, C. (2008). A Review on buildings energy consumption information. *Energy and Buildings*, *40*, 394-398. https://doi.org/10.1016/j.enbuild.2007.03.007

Pope, M. A., Korkut, S., Punckt, C., & Aksay, I. A. (2013). Supercapacitor Electrodes Produced through Evaporative Consolidation of Graphene Oxide-Water-Ionic Liquid Gels. *Journal of the Electrochemical Society*, *160*(10), A1653. https://doi.org/10.1149/2.017310jes

Pu, X., Ren, X., Yin, H., Tang, Y., & Yuan, H. (2021). One-step electrodeposition strategy for growing nickel cobalt hydroxysulfide nanosheets for supercapacitor application. *Journal of Alloys and Compounds*, *865*, 158736.

Qu, D. (2002). Studies of the activated carbons used in double-layer supercapacitors. *Journal of power sources*, *109*(2), 403-411. https://doi.org/https://doi.org/10.1016/S0378-7753(02)00108-8

Ragupathy, P., Park, D., Campet, G., Vasan, H., Hwang, S.-J., Choy, J.-H., & Nookala, M. (2009). Remarkable Capacity Retention of Nanostructured Manganese Oxide upon Cycling as an Electrode Material for Supercapacitor. *Journal of Physical Chemistry C - J PHYS CHEM C*, *113*. https://doi.org/10.1021/jp811407q

Ramasubramanian, B., Chinglenthoiba, C., Huiqing, X., Xiping, N., Hui, H. K., Valiyaveettil, S., Ramakrishna, S., & Chellappan, V. (2022). Sustainable Fe-MOF@carbon nanocomposite electrode for supercapacitor. *Surfaces and Interfaces*, *34*, 102397. https://doi.org/https://doi.org/10.1016/j.surfin.2022.102397

Raza, W., Ali, F., Raza, N., Luo, Y., Kim, K.-H., Yang, J., Kumar, S., Mehmood, A., & Kwon, E. E. (2018). Recent advancements in supercapacitor technology. *Nano Energy*, *52*, 441-473. https://doi.org/10.1016/j.nanoen.2018.08.013

Ren, L., Wu, Q., Yang, C., Zhu, L., Li, C., Zhang, P., Zhang, H., Meng, X., & Xiao, F. S. (2012). Solvent-free synthesis of zeolites from solid raw materials. *J Am Chem Soc*, *134*(37), 15173-15176. https://doi.org/10.1021/ja3044954

Ribeiro, P. F., Johnson, B. K., Crow, M. L., Arsoy, A., & Liu, Y. (2001). Energy storage systems for advanced power applications. *Proceedings of the IEEE*, *89*(12), 1744-1756. https://doi.org/10.1109/5.975900

Sb, M. (2015). Building Energy Consumption and Carbon dioxide Emissions: Threat to Climate Change. *Journal of Earth Science & Climatic Change*, *s3*. https://doi.org/10.4172/2157-7617.S3-001

Schneuwly, A., & Gallay, R. (2000). *Properties and Applications of Supercapacitors From the State-of-the-art to Future Trends*.

Shafiei, M., Alivand, M. S., Rashidi, A., Samimi, A., & Mohebbi-Kalhori, D. (2018). Synthesis and adsorption performance of a modified micro-mesoporous MIL-101 (Cr)

for VOCs removal at ambient conditions. *Chemical Engineering Journal*, *341*, 164-174.

Sichumsaeng, T., Chanlek, N., & Maensiri, S. (2018). Effect of various electrolytes on the electrochemical properties of Ni(OH)2 nanostructures. *Applied Surface Science*, *446*, 177-186. https://doi.org/10.1016/j.apsusc.2018.01.276

Simon, P., & Gogotsi, Y. (2008). Materials for electrochemical capacitors. *Nat Mater*, *7*(11), 845-854. https://doi.org/10.1038/nmat2297

Simon, P., & Gogotsi, Y. (2008). Materials for electrochemical capacitors. *Nature Materials*, *7*(11), 845-854. https://doi.org/10.1038/nmat2297

Simon, P., & Gogotsi, Y. (2013). Capacitive Energy Storage in Nanostructured Carbon–Electrolyte Systems. *Accounts of Chemical Research*, *46*(5), 1094-1103. https://doi.org/10.1021/ar200306b

Sivanantham, K., Narenthiran, B., Sivanantham, A., Bhatlu M, L. D., & Maridurai, T. (2021). Supercapacitor: Evolution and review. *Materials Today: Proceedings*, *46*. https://doi.org/10.1016/j.matpr.2021.02.526

Snook, G. A., Kao, P., & Best, A. S. (2011). Conducting-polymer-based supercapacitor devices and electrodes. *Journal of power sources*, *196*(1), 1-12. https://doi.org/https://doi.org/10.1016/j.jpowsour.2010.06.084

Soltani, M., Dehghani-Sanij, A., Sayadnia, A., Kashkooli, F. M., Gharali, K., Mahbaz, S., & Dusseault, M. B. (2018). Investigation of Airflow Patterns in a New Design of Wind Tower with a Wetted Surface. *Energies*, *11*(5), 1100. https://www.mdpi.com/1996-1073/11/5/1100

Song, Z., Hou, J., Hofmann, H., Li, J., & Ouyang, M. (2017). Sliding-mode and Lyapunov function-based control for battery/supercapacitor hybrid energy storage system used in electric vehicles. *Energy*, *122*, 601-612.

Sotnik, S. A., Gavrilenko, K. S., Lytvynenko, A. S., & Kolotilov, S. V. (2015). Catalytic activity of copper (II) benzenetricarboxylate (HKUST-1) in reactions of aromatic aldehydes condensation with nitromethane: Kinetic and diffusion study. *Inorganica Chimica Acta*, *426*, 119-125.

Stoller, M. D., Park, S., Zhu, Y., An, J., & Ruoff, R. S. (2008). Graphene-based ultracapacitors. *Nano letters*, *8*(10), 3498-3502.

Sugimoto, W. (2014). Ruthenium Oxides as Supercapacitor Electrodes. In G. Kreysa, K.-i. Ota, & R. F. Savinell (Eds.), *Encyclopedia of Applied Electrochemistry* (pp. 1813-1821). Springer New York. https://doi.org/10.1007/978-1-4419-6996-5_511

Sun, L., Cai, Y., Haider, M. K., Miyagi, D., Zhu, C., & Kim, I. S. (2022). Structural design and optimization of metal-organic framework-derived FeOx@C/rGO anode materials for constructing high-performance hybrid supercapacitors. *Composites Part B: Engineering*, *236*, 109812. https://doi.org/https://doi.org/10.1016/j.compositesb.2022.109812

Sun, Z., Peng, Y., Wang, M., Lin, Y., Jalalah, M., Alsareii, S. A., Harraz, F. A., Yang, J., & Li, G. (2021). Electrochemical deposition of Cu metal–organic framework films for the dual analysis of pathogens. *Analytical Chemistry*, *93*(25), 8994-9001.

Sundriyal, S., Kaur, H., Bhardwaj, S. K., Mishra, S., Kim, K.-H., & Deep, A. (2018). Metal-organic frameworks and their composites as efficient electrodes for supercapacitor applications. *Coordination Chemistry Reviews*, *369*, 15-38. https://doi.org/10.1016/j.ccr.2018.04.018

Tasnin, W., & Saikia, L. C. (2018). Performance comparison of several energy storage devices in deregulated AGC of a multi-area system incorporating geothermal power plant. *IET Renewable Power Generation*, *12*(7), 761-772.

Tonelli, D., Gualandi, I., Musella, E., & Scavetta, E. (2021). Synthesis and Characterization of Layered Double Hydroxides as Materials for Electrocatalytic Applications. *Nanomaterials*, *11*, 725. https://doi.org/10.3390/nano11030725

Tranchemontagne, D. J., Mendoza-Cortés, J. L., O'keeffe, M., & Yaghi, O. M. (2009). Secondary building units, nets and bonding in the chemistry of metal–organic frameworks. *Chemical Society Reviews*, *38*(5), 1257-1283.

Trung, T. K., Ramsahye, N. A., Trens, P., Tanchoux, N., Serre, C., Fajula, F., & Férey, G. (2010). Adsorption of C5–C9 hydrocarbons in microporous MOFs MIL-100 (Cr) and MIL-101 (Cr): A manometric study. *Microporous and mesoporous materials*, *134*(1-3), 134-140.

Walton, R. I., Munn, A. S., Guillou, N., & Millange, F. (2011). Uptake of Liquid Alcohols by the Flexible FeIII Metal–Organic Framework MIL-53 Observed by Time-Resolved In

Situ X-ray Diffraction. *Chemistry – A European Journal*, *17*(25), 7069-7079. https://doi.org/https://doi.org/10.1002/chem.201003634

Wang, D., Wei, A., Tian, L., Mensah, A., Li, D., Xu, Y., & Wei, Q. (2019). Nickel-cobalt layered double hydroxide nanosheets with reduced graphene oxide grown on carbon cloth for symmetric supercapacitor. *Applied Surface Science*, *483*. https://doi.org/10.1016/j.apsusc.2019.03.345

Wang, G., Zhang, L., & Zhang, J. (2012). A review of electrode materials for electrochemical supercapacitors. *Chemical Society Reviews*, *41*(2), 797-828.

Wang, H., Yang, Y., Liang, Y., Robinson, J. T., Li, Y., Jackson, A., Cui, Y., & Dai, H. (2011). Graphene-wrapped sulfur particles as a rechargeable lithium-sulfur battery cathode material with high capacity and cycling stability. *Nano Lett*, *11*(7), 2644-2647. https://doi.org/10.1021/nl200658a

Wang, J., Liu, W., Luo, G., Li, Z., Zhao, C., Zhang, H., Zhu, M., Xu, Q., Wang, X., Zhao, C., Qu, Y., Yang, Z., Yao, T., Li, Y., Lin, Y., Wu, Y., & Li, Y. (2018). Synergistic effect of well-defined dual sites boosting the oxygen reduction reaction [10.1039/C8EE02656D]. *Energy & Environmental Science*, *11*(12), 3375-3379. https://doi.org/10.1039/C8EE02656D

Wang, M., Ma, Y., & Ye, J. (2020). Controllable layer-by-layer assembly of metal-organic frameworks/polyaniline membranes for flexible solid-state microsupercapacitors. *Journal of Power Sources*, *474*, 228681.

Wang, S., & Jiang, S. P. (2017). Prospects of fuel cell technologies. *National Science Review*, *4*(2), 163-166.

Wang, Y., Shi, Z., Huang, Y., Ma, Y., Wang, C., Chen, M., & Chen, Y. (2009). Supercapacitor Devices Based on Graphene Materials. *The Journal of Physical Chemistry C*, *113*(30), 13103-13107. https://doi.org/10.1021/jp902214f

Wee, L. H., Janssens, N., Bajpe, S. R., Kirschhock, C. E., & Martens, J. A. (2011). Heteropolyacid encapsulated in Cu3 (BTC) 2 nanocrystals: An effective esterification catalyst. *Catalysis Today*, *171*(1), 275-280.

Weiss, M., Ruess, R., Kasnatscheew, J., Levartovsky, Y., Levy, N. R., Minnmann, P., Stolz, L., Waldmann, T., Wohlfahrt-Mehrens, M., & Aurbach, D. (2021). Fast charging of

lithium-ion batteries: a review of materials aspects. *Advanced Energy Materials*, *11*(33), 2101126.

White, R. J., Budarin, V. L., & Shuttleworth, P. S. (2015). Other Approaches and the Commercialisation of Sustainable Carbonaceous Material Technology. In R. J. White (Ed.), *Porous Carbon Materials from Sustainable Precursors* (pp. 0). The Royal Society of Chemistry. https://doi.org/10.1039/9781782622277-00377

Winter, M., Besenhard, J. O., Spahr, M. E., & Novak, P. (1998). Insertion electrode materials for rechargeable lithium batteries. *Advanced Materials*, *10*(10), 725-763.

Winter, M., & Brodd, R. J. (2004). What are batteries, fuel cells, and supercapacitors? *Chemical Reviews*, *104*(10), 4245-4270.

Winter, M., & Brodd, R. J. (2004). What are batteries, fuel cells, and supercapacitors? *Chem Rev*, *104*(10), 4245-4269. https://doi.org/10.1021/cr020730k

Wu, H., He, D., Wang, Y., Fu, M., Liu, Z., Wang, J., & Wang, H. (2010). Graphene as the electrode material in supercapacitors. 2010 8th International vacuum electron sources Conference and Nanocarbon,

Xiaobo, M., Xinyu, L., Jie, Z., Xiaoxian, H., & Weichun, Y. (2021). Heterostructured TiO(2)@HKUST-1 for the enhanced removal of methylene blue by integrated adsorption and photocatalytic degradation. *Environ Technol*, *42*(26), 4134-4144. https://doi.org/10.1080/09593330.2020.1745295

Xie, L., Liu, S., Han, Z., Jiang, R., Liu, H., Zhu, F., Zeng, F., Su, C., & Ouyang, G. (2015). Preparation and characterization of metal-organic framework MIL-101 (Cr)-coated solid-phase microextraction fiber. *Analytica Chimica Acta*, *853*, 303-310.

Xiong, R., Pan, Y., Shen, W., Li, H., & Sun, F. (2020). Lithium-ion battery aging mechanisms and diagnosis method for automotive applications: Recent advances and perspectives. *Renewable and Sustainable Energy Reviews*, *131*, 110048. https://doi.org/https://doi.org/10.1016/j.rser.2020.110048

Xiong, S., Lin, X., Liu, S., Weng, S., Jiang, S., Jiao, Y., Xu, Y., & Cheng, J. (2020). Metal-organic framework derived α-Fe2O3 nano-octahedron with oxygen vacancies for realizing outstanding energy storage performance. *Vacuum*, *182*, 109692. https://doi.org/https://doi.org/10.1016/j.vacuum.2020.109692

Xu, K. (2004). Nonaqueous Liquid Electrolytes for Lithium-Based Rechargeable Batteries. *Chemical Reviews*, *104*(10), 4303-4418. https://doi.org/10.1021/cr030203g

Yadav, S., & Sharma, A. (2021). Importance and challenges of hydrothermal technique for synthesis of transition metal oxides and composites as supercapacitor electrode materials. *Journal of Energy Storage*, *44*, 103295.

Yang, Q., Xue, C., Zhong, C., & Chen, J. F. (2007). Molecular simulation of separation of CO2 from flue gases in CU-BTC metal-organic framework. *AIChE journal*, *53*(11), 2832-2840.

Yepez, R., García, S., Schachat, P., Sánchez-Sánchez, M., González-Estefan, J. H., González-Zamora, E., Ibarra, I. A., & Aguilar-Pliego, J. (2015). Catalytic activity of HKUST-1 in the oxidation of trans-ferulic acid to vanillin. *New Journal of Chemistry*, *39*(7), 5112-5115.

Yu, X., Yu, Z.-Y., Zhang, X.-L., Li, P., Sun, B., Gao, X., Yan, K., Liu, H., Duan, Y., Gao, M.-R., Wang, G., & Yu, S.-H. (2020). Highly disordered cobalt oxide nanostructure induced by sulfur incorporation for efficient overall water splitting. *Nano Energy*, *71*, 104652. https://doi.org/https://doi.org/10.1016/j.nanoen.2020.104652

Yu, X., Yun, S., Yeon, J. S., Bhattacharya, P., Wang, L., Lee, S. W., Hu, X., & Park, H. S. (2018). Emergent Pseudocapacitance of 2D Nanomaterials. *Advanced Energy Materials*, *8*(13), 1702930. https://doi.org/https://doi.org/10.1002/aenm.201702930

Yuan, S., Xian, Y., Long, Y., Cabot, A., Li, W., & Fan, J. (2021). Chromium-Based Metal–Organic Framework as A-Site Cation in CsPbI2Br Perovskite Solar Cells. *Advanced Functional Materials*, *31*(51), 2106233. https://doi.org/https://doi.org/10.1002/adfm.202106233

Zhang, J.-j., Zhang, T.-a., & Feng, S. (2020). α-Ni(OH)2 electrodeposition from NiCl2 solution. *Transactions of Nonferrous Metals Society of China*, *30*(10), 2802-2811. https://doi.org/https://doi.org/10.1016/S1003-6326(20)65422-X

Zhang, M., Chen, Y., Yang, D., & Li, J. (2020). High performance MnO2 supercapacitor material prepared by modified electrodeposition method with different electrodeposition voltages. *Journal of Energy Storage*, *29*, 101363.

Zhang, R., Xu, Y., Harrison, D., Fyson, J., Southee, D., & Tanwilaisiri, A. (2015). Fabrication and Characterisation of Smart Fabric Using Energy Storage Fibres. *Systems Science & Control Engineering*, *3*, 1-6. https://doi.org/10.1080/21642583.2015.1049717

Zhang, X., Wan, K., Subramanian, P., Xu, M., Luo, J., & Fransaer, J. (2020). Electrochemical deposition of metal–organic framework films and their applications. *Journal of materials chemistry A*, *8*(16), 7569-7587.

Zhang, Y., Wang, Y., Cheng, T., Lai, W., Pang, H., & Huang, W. (2015). Flexible supercapacitors based on paper substrates: a new paradigm for low-cost energy storage. *Chemical Society Reviews*, *44*. https://doi.org/10.1039/c5cs00174a

Zhang, Z., Wang, Y., Jia, X., Yang, J., & Li, J. (2017). The synergistic effect of oxygen and water on the stability of the isostructural family of metal–organic frameworks [Cr 3 (BTC) 2] and [Cu 3 (BTC) 2]. *Dalton Transactions*, *46*(44), 15573-15581.

Zhao, G., Chen, C., Yu, D., Sun, L., Yang, C., Zhang, H., Sun, Y., Besenbacher, F., & Yu, M. (2018). One-step production of O-N-S co-doped three-dimensional hierarchical porous carbons for high-performance supercapacitors. *Nano Energy*, *47*, 547-555. https://doi.org/https://doi.org/10.1016/j.nanoen.2018.03.016

Zhaojin Li, Q. L., Lizhi Sun, Ning Li, Xiaofeng Wang, Qiujun Wang, Di Zhang, Bo Wang,. (2022). Hydrothermal synthesis of 3D hierarchical ordered porous carbon from yam biowastes for enhanced supercapacitor performance. *Chemical Engineering Science*, *252*. https://doi.org/10.1016/j.ces.2022.117514

Zhu, M., Huang, Y., Huang, Y., Meng, W., Gong, Q., Li, G., & Zhi, C. (2015). An electrochromic supercapacitor and its hybrid derivatives: quantifiably determining their electrical energy storage by an optical measurement [10.1039/C5TA06237C]. *Journal of materials chemistry A*, *3*(42), 21321-21327. https://doi.org/10.1039/C5TA06237C

Zhu, Y., Su, P., Wang, J., & Wang, X. (2023). Research Progress on Metal–Organic Framework-Based Electrode Materials for Supercapacitors. *Crystals*, *13*(11). https://doi.org/10.3390/cryst13111593